International Journal of Earth Sciences
https://doi.org/10.1007/s00531-022-02278-y

ORIGINAL PAPER

Two distinct age groups of melilitites, foidites, and basanites from the southern Central European Volcanic Province reflect lithospheric heterogeneity

Thomas Binder[1] · Michael A. W. Marks[1] · Axel Gerdes[2,3] · Benjamin F. Walter[4,5] · Jens Grimmer[4] · Aratz Beranoaguirre[2,3,4,5] · Thomas Wenzel[1] · Gregor Markl[1]

Received: 21 December 2021 / Accepted: 22 November 2022

Abstract

Petrographic observations and in situ U–Pb ages of melilitites, foidites, basanites, phonolites, and trachytes from the southern part of the Central European Volcanic Province (CEVP) and related plutonic inclusions therein reveal two distinct age groups separated by a gap of ~ 20 Myr. A late Cretaceous to early Eocene group (~ 73–47 Ma; Taunus, Lower Main plain, Odenwald and Kraichgau area, Bonndorfer Graben and Freiburger Bucht area, Vosges and Pfälzerwald) is characterized by nephelinites and basanites mostly devoid of melilite and perovskite, and by rare haüynites, and trachytes. In contrast, a late Oligocene to late Miocene group (~ 27–9 Ma; Lorraine, southern Upper Rhine Graben, Urach, Hegau area) is dominated by melilitites, melilite-bearing nephelinites (both carrying perovskite), and phonolites. Both magmatic episodes are related to domal topographic uplift, erosion, and formation of major angular unconformities in the Upper Rhine Graben, suggesting an association with dynamic topography interrupted by phases of subsidence (or abatements of uplift). The investigated rocks in the southern CEVP (south of a line Eifel–Vogelsberg–Rhön–Heldburg), except for the Kaiserstuhl volcanic complex, mostly comprise small and isolated occurrences or monogenetic volcanic fields, whereas the northern CEVP is dominated by large volcanic complexes and dyke swarms, which are mostly SiO_2-saturated to weakly SiO_2-undersaturated. In the northern CEVP, evidence of spatially varying but recurrent volcanic activity exists since the Eocene, lacking the distinct 20 Myr gap as documented from the southern CEVP. While the temporal and spatial distribution of volcanism are a result of the Cretaceous to Miocene tectonic evolution in Central Europe, further studies are needed to explain the petrographic differences between the two age groups in the south.

Keywords In situ U–Pb dating · Central European Volcanic Province · Upper Rhine Graben · Foidites · Olivine melilitites · Geochronology of volcanic rocks

✉ Thomas Binder
thomas.binder@uni-tuebingen.de

[1] Department of Geosciences, Eberhard Karls Universität Tübingen, Schnarrenbergstraße 94–96, 72076 Tübingen, Germany

[2] Frankfurt Isotope and Element Research Center (FIERCE), Goethe-Universität Frankfurt, Altenhöferallee 1, 60438 Frankfurt am Main, Germany

[3] Department of Geosciences, Goethe-Universität Frankfurt, Altenhöferallee 1, 60438 Frankfurt am Main, Germany

[4] Institute of Applied Geosciences, Karlsruhe Institute of Technology, Adenauerring 20b, 76131 Karlsruhe, Germany

[5] Laboratory for Environmental and Raw Material Analysis (LERA), Adenauerring 20b, 76131 Karlsruhe, Germany

Introduction

The late Cretaceous–Holocene Central European Volcanic Province (CEVP; Fig. 1, Table 1) is part of the Circum-Mediterranean Anorogenic Cenozoic Igneous province (CiMACI; Lustrino and Wilson 2007) and comprises several volcanic regions in eastern France, western, central, and southern Germany, western Poland, and the Czech Republic (e.g., Lustrino and Wilson 2007; Schmitt et al. 2007; Sirocko et al. 2013). Many of these regions are characterized by polygenetic, others by monogenetic igneous activities. Some of them comprise large-scale lava sheets or pyroclastic deposits, while others consist of accumulations of vents, stocks, or dykes. The volcanic products investigated in the studied area (Table 1) comprise basalts, basanites, tephrites,

Published online: 04 December 2022

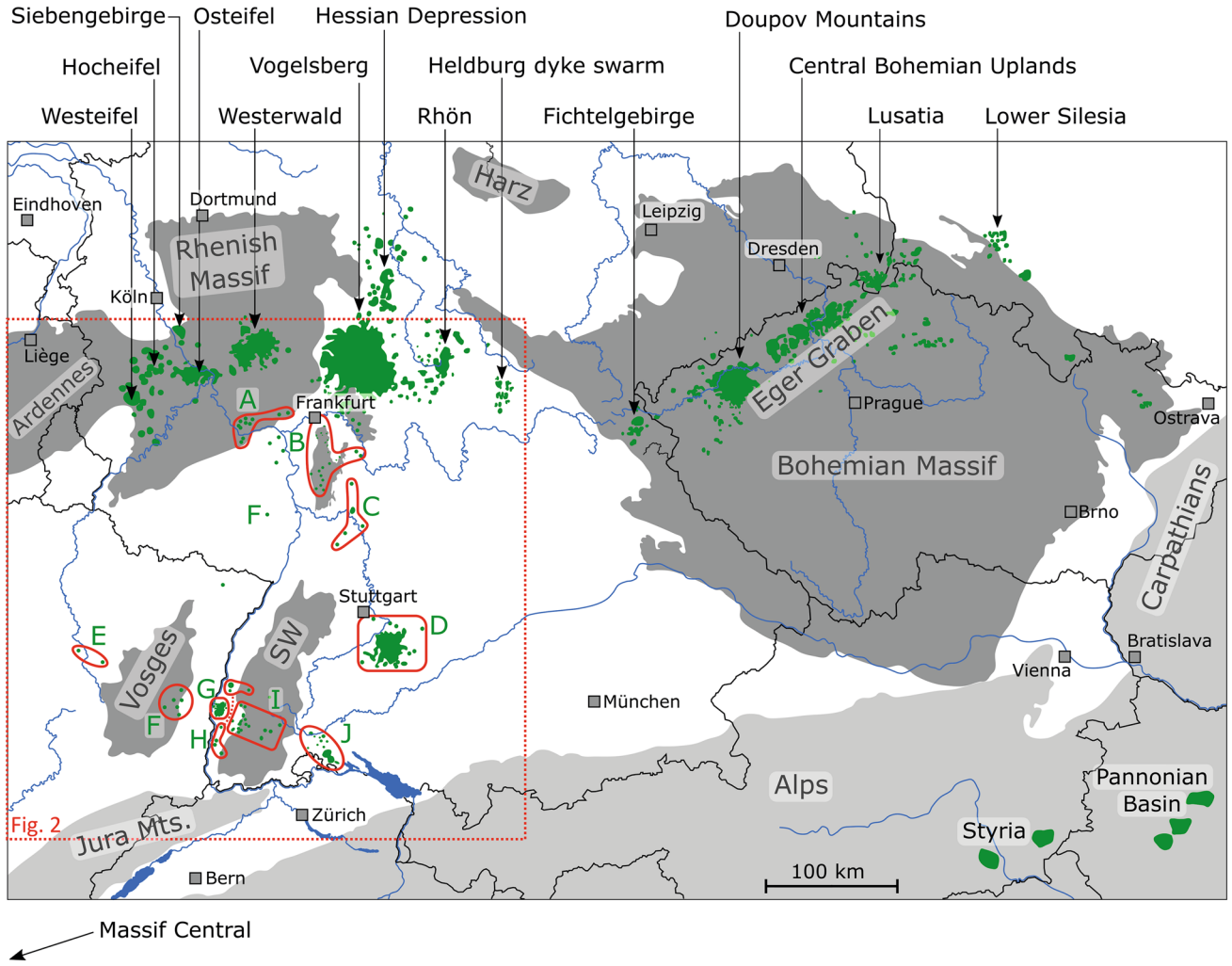

Fig. 1 Map showing the Central European Volcanic Province (CEVP) with their volcanic fields and complexes in green. Variscan basement rocks are shown in dark grey, rocks affected by the Alpine orogeny in light grey. The study areas of this work are outlined in red. *A* Taunus, *B* Lower Main plain, *C* Odenwald and Kraichgau area, *D* Urach, *E* Lorraine, *F* Vosges and Pfälzerwald, *G* Kaiserstuhl, *H* Southern Upper Rhine Graben, *I* Bonndorfer Graben and Freiburger Bucht area, *J* Hegau area

Table 1 Geomorphological characteristics and number of known localities within the regions in the southern CEVP (study area)

Region	Plugs/necks	Dykes	Tuff diatremes	*n*
Hegau area (J)	++	+	o	~30 and extensive tuff
Urach (D)	+	+	++	>400
Kaiserstuhl (G)	Stratovolcanic complex			
Southern URG (H)	+	+	+	13
Lorraine (E)	++	o	o	2
Vosges and Pfälzerwald (F)	++	o	+	10
Taunus (A)	++		+	~15
Bonndorfer Graben and Freiburger Bucht (I)	++	+	+	~30
Odenwald and Kraichgau area (C)	++	o	o	8
Lower Main plain (B)	++	o	+	~30

n number of known occurrences; ++ abundant; + present; o: absent; letters in brackets refer to the areas illustrated in Figs. 1, 2, 4, 7, and 8)

latites, trachytes, phonolites, nephelinites, haüynites, melilitites, and carbonatites (e.g., Abratis et al. 2009; Bogaard and Wörner 2003; Braunger et al. 2018; Büchner et al. 2015; Dunworth and Wilson 1998; Jung and Hoernes 2000; Jung et al. 2005, 2006, 2011; Kolb et al. 2012; Kramm and Wedepohl 1990; Schubert et al. 2015; Skála et al. 2015; Ulrych et al. 2016; Wörner et al. 1986).

The volcanic activity in the CEVP is closely related to the evolution of the European Cenozoic Rift System (ECRiS; e.g., Dèzes et al. 2004; Merle 2011), in particular to the changes in the Alpine foreland stress field and the local reactivation of Variscan-age lithosphere-scale faults (Dèzes et al. 2004; Goes et al. 1999). The relationship between uplift, rifting, and volcanism in Central Europe is controversial, and several competing and complementary models of melt generation and melt sources have been proposed (e.g., Goes et al. 1999; Lustrino and Wilson 2007; Pfänder et al. 2018 and references therein). Explanations range from asthenospheric mantle upwelling caused by thermal instabilities (active upwelling) to melt formation by lithospheric deformation and thinning (passive rifting), both resulting in decompression melting (Lustrino and Wilson 2007; Pfänder et al. 2018; Ulrych et al. 2013). For the former case, an active large-scale mantle plume system, anchored near the core–mantle boundary layer (e.g., Albers and Christensen 1996; Goes et al. 1999), or several smaller (finger-like) plumes sourced in the asthenosphere or the transition zone have been proposed as the cause for magmatism (e.g., Dèzes et al. 2004; Goes et al. 1999; Granet et al. 1995; Haase et al. 2004; Hegner et al. 1995; Mertz et al. 2015; Ritter et al. 2001; Wedepohl and Baumann 1999). Opposing concepts that reject the dominant influence of mantle plumes invoke a partly metasomatized upper mantle beneath the CEVP that interacted with fluids and/or melts derived from subducted ancient oceanic and continental lithosphere, resulting in the presence of (low-melting) hydrous and partly carbonate-bearing mantle domains (Blusztajn and Hegner 2002; Jung et al. 2005; Pfänder et al. 2018; Ulrych et al. 2008). Such models assume that decompression and subsequent melt formation are primarily caused by passive asthenospheric upwelling as a result of lithospheric thinning, uplift, and erosion (Eynatten et al. 2021; Fichtner and Villaseñor 2015; Lustrino and Carminati 2007).

Considering the variable composition, the different ages and magma volumes, and the occasional lack of spatial correlation between volcanism, graben structures, and thinned lithosphere for CEVP volcanic activity (Dunworth and Wilson 1998; Goes et al. 1999; Pfänder et al. 2018), it seems likely that a single general model alone cannot explain the petrogenesis of all the occurrences (Eynatten et al. 2021; Lustrino and Wilson 2007; Mertz et al. 2015). Rather, the spatial chemical heterogeneity of the lower lithospheric mantle, the formation depth and origin of the magmas, and the varying position of the lithosphere–asthenosphere boundary must be integrated into a comprehensive geodynamic scenario (Lustrino and Carminati 2007; Lustrino and Wilson 2007; Puziewicz et al. 2020).

In the northern part of the CEVP, numerous occurrences of volcanic rocks have been dated by modern $^{40}Ar/^{39}Ar$ techniques (e.g., Abratis et al. 2007; Büchner et al. 2015; Linthout et al. 2009; Mayer et al. 2014; Mertz et al. 2000, 2007, 2015; Pfänder et al. 2018; Przybyla et al. 2018; Schubert et al. 2015; Shaw et al. 2010; Singer et al. 2008; van den Bogaard 1995). In the southern CEVP, however, modern geochronological studies are rare (Fekiacova et al. 2007; Keller et al. 2002; Schmitt et al. 2007) and precise ages for many regions and individual localities in the southern CEVP are still lacking and existing ages mostly represent old K–Ar whole-rock data (Baranyi et al. 1976; Horn et al. 1972; Lippolt et al. 1963, 1973, 1975; Lippolt 1983), which have been shown to be erroneous or at least imprecise in several cases (e.g., Baranyi et al. 1976; Keller et al. 2002; Lippolt et al. 1963).

Here, we present a detailed study on primitive to evolved, mostly SiO_2-undersaturated rocks of the southern CEVP applying in situ U–Pb dating of the magmatic phases perovskite, apatite, titanite, zircon, and pyrochlore using LA-ICP-MS analyses on samples carefully studied petrographically. Considering the observed spatial and compositional variations, the present study not only contributes to understanding the chronology of magmatism in the CEVP, but provides also inferences on the driving forces responsible for the volcanic activity, regarding its close link to the preceding melting processes in the upper mantle.

Geological setting

The northern part of the CEVP comprises larger volcanic fields and dyke swarms of the Eifel, Siebengebirge, Westerwald, Vogelsberg, Hessian Depression, Rhön, Heldburg region, Fichtelgebirge, Doupov Mountains, Central Bohemian Uplands, Lusatia, and Lower Silesia (Fig. 1). The focus of the present study is the southern part of the CEVP encompassing volcanic rocks in the Taunus, Lower Main plain, Odenwald and Kraichgau area, Bonndorfer Graben and Freiburger Bucht area, Vosges and Pfälzerwald, Lorraine, southern Upper Rhine Graben (URG), at Urach, and in the Hegau area (Fig. 1, Online Resource 1). The volcanic rocks of Urach, the Hegau area, the southern URG, and Lorraine are strongly SiO_2-undersaturated and comprise primitive olivine melilitites, melilite-bearing olivine nephelinites, and evolved phonolites, contrasting with melilite-free olivine nephelinites, basanitic nephelinites, nepheline basanites, haüynites, and trachytes in the remaining regions (Figs. 2 and 3).

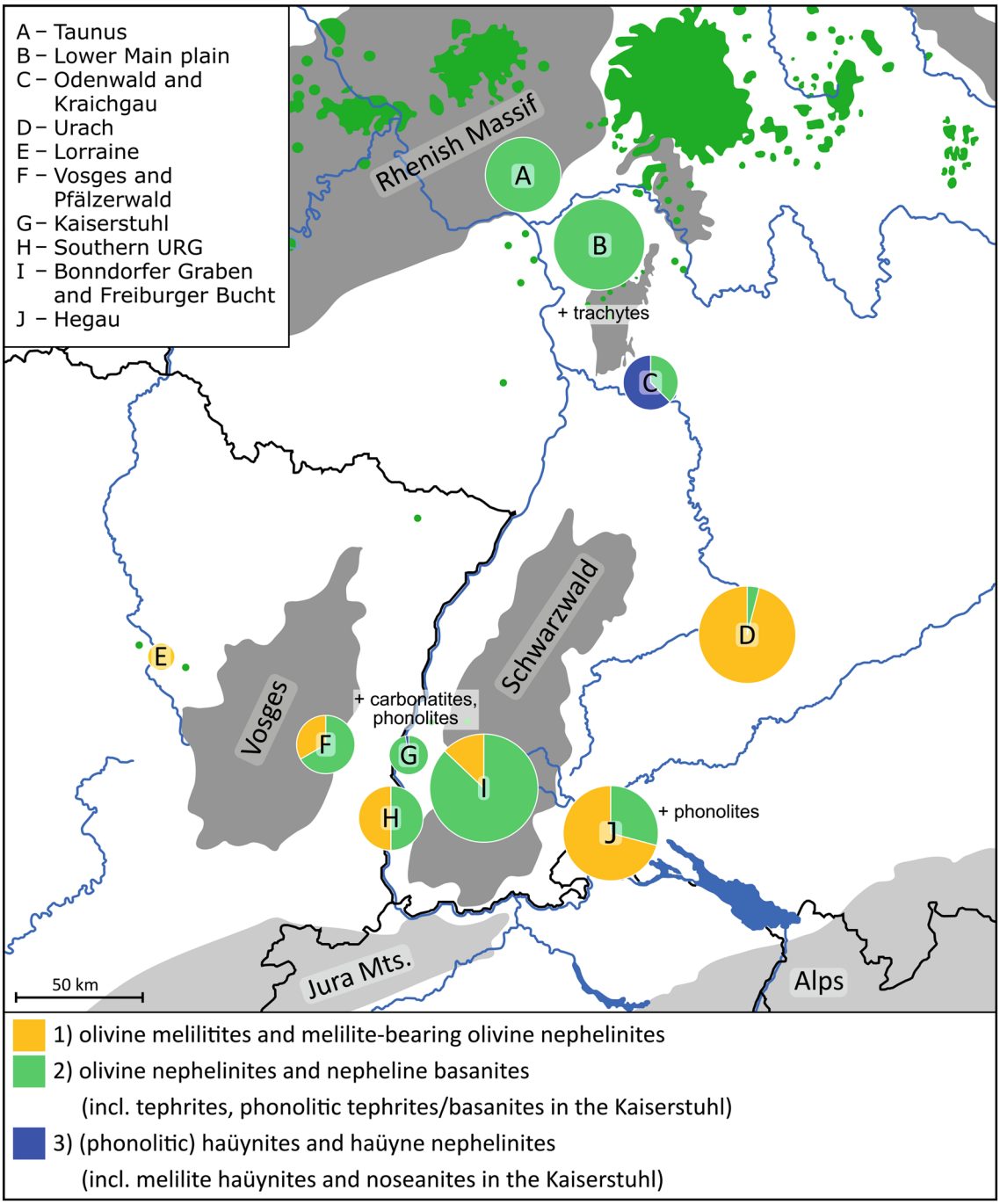

Fig. 2 Map of SW Germany and E France showing the study areas of this work as circular diagrams representing the semi-quantitative distribution of groups of SiO_2-undersaturated rock types in each region determined by number of known occurrences. The circle size roughly correlates with the number of described occurrences (Lorraine: $n = 2$, Bonndorfer Graben and Freiburger Bucht area: $n = 31$), except for the Kaiserstuhl, for which surface coverage percentages are used. The rock types were determined by microscopy of 215 thin sections from approx. 120 localities in the southern CEVP. For regions that also contain strongly evolved rocks, these are additionally stated

Most of the studied occurrences are tied to obvious tectonic structures (Fig. 4): the Kaiserstuhl volcanic complex and several isolated stocks and diatremes are located within the URG between the Variscan massifs of the Vosges and the Schwarzwald. The volcanic dykes and vents in these massifs occur on the flanks of the URG (e.g., Freiburger Bucht) and in the WNW-trending Bonndorfer Graben, merging eastwards into the Hegau Graben that hosts additional dykes, plugs, domes, and larger tuff deposits. The Albstadt shear zone is a seismically active, few km wide, deformation zone

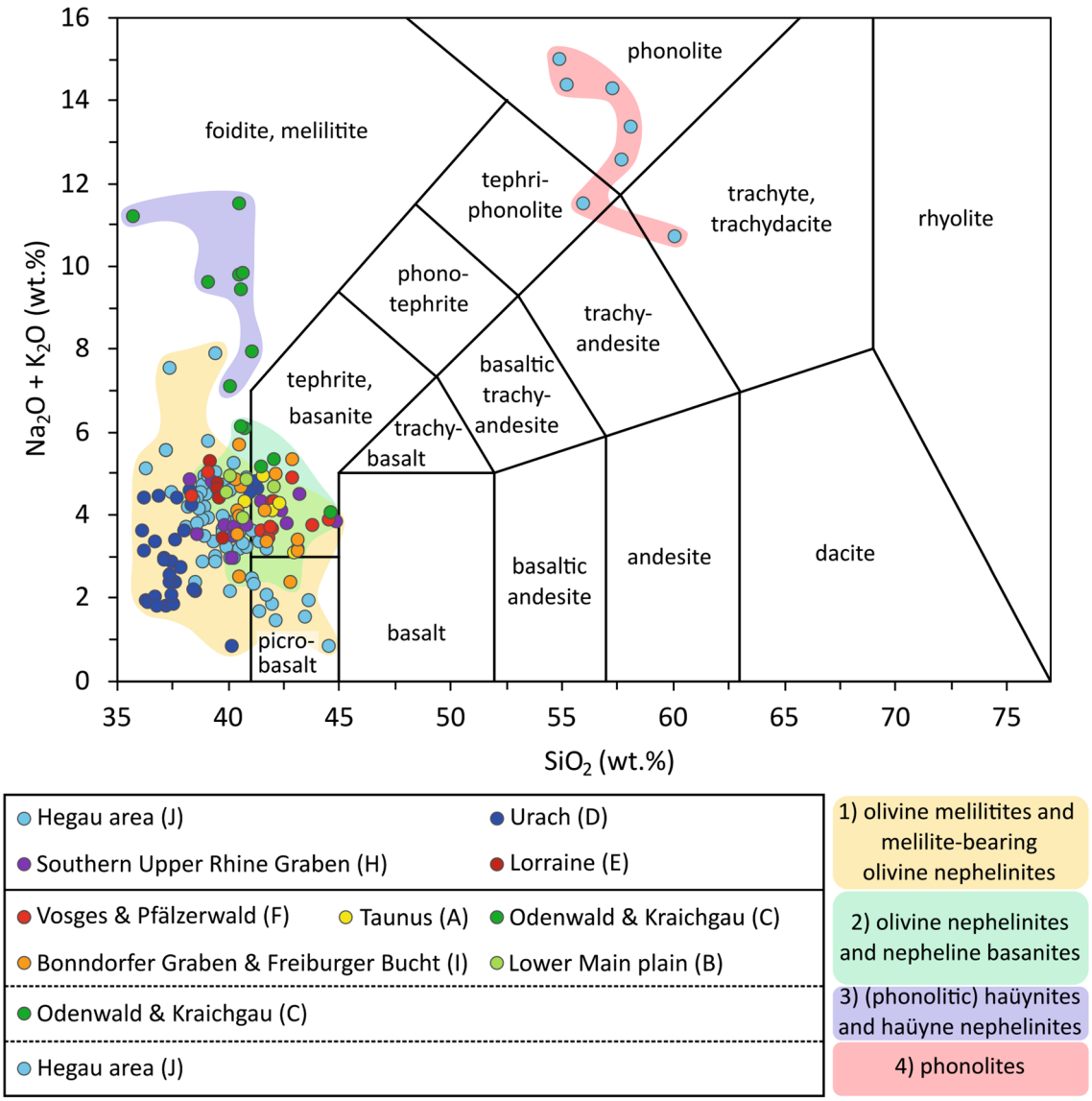

Fig. 3 TAS diagram for the investigated rocks in the southern CEVP. Thirty-four new analyses performed according to the XRF method reported in Braunger et al. (2018) were supplemented by literature data from Dunworth and Wilson (1998), Frenzel (1975), Hegner et al. (1995), Hurrle (1976), Keller et al. (1990), Krause and Weiskirchner (1981), Neumann et al. (1992), Staesche (1995), Stähle and Koch (2003), and Stellrecht and Emmermann (1970). All data have been renormalized to a volatile-free composition. Note that the naming of the rocks in the petrography chapter was done based on the mineral composition, which is why the position in the TAS diagram may differ from the assigned rock name. No whole-rock analyses are available for the trachytes of the Lower Main plain

(Mader et al. 2021) that trends parallel to the URG and connects the Hegau Graben with the westernmost margin of the Urach volcanic field, which is delimited by several minor faults (Fig. 4; Ring and Bolhar 2020). The volcanic rocks of the Lower Main plain occur along the eastern flank of the URG (Sprendlinger Horst), those from Forst (Pfälzerwald) and the more southerly Vosges along the western flank. The basanites and nephelinites in the Taunus trend parallel to the South Hunsrück–Taunus border fault, while the volcanic rocks in the Odenwald and Kraichgau area and Lorraine are not associated with any obvious structure.

The study area comprises some of the most primitive melilitites and nephelinites of the entire CEVP (Fig. 3). However, while several studies on the petrogenesis of such rocks exist for the northern part of the CEVP (e.g., Duda and Schmincke 1985; Harmon et al. 1987; Jung et al. 2006; Pfänder et al. 2018; Skála et al. 2015; Ulrych et al. 2008, 2011, 2013, 2016), similar occurrences in the southern CEVP have been much less investigated (Blusztajn and Hegner 2002; Dunworth and Wilson 1998; Hegner et al. 1995; Hegner and Vennemann 1997) and comparative work involves SiO_2-saturated, basaltic and evolved rocks (e.g.,

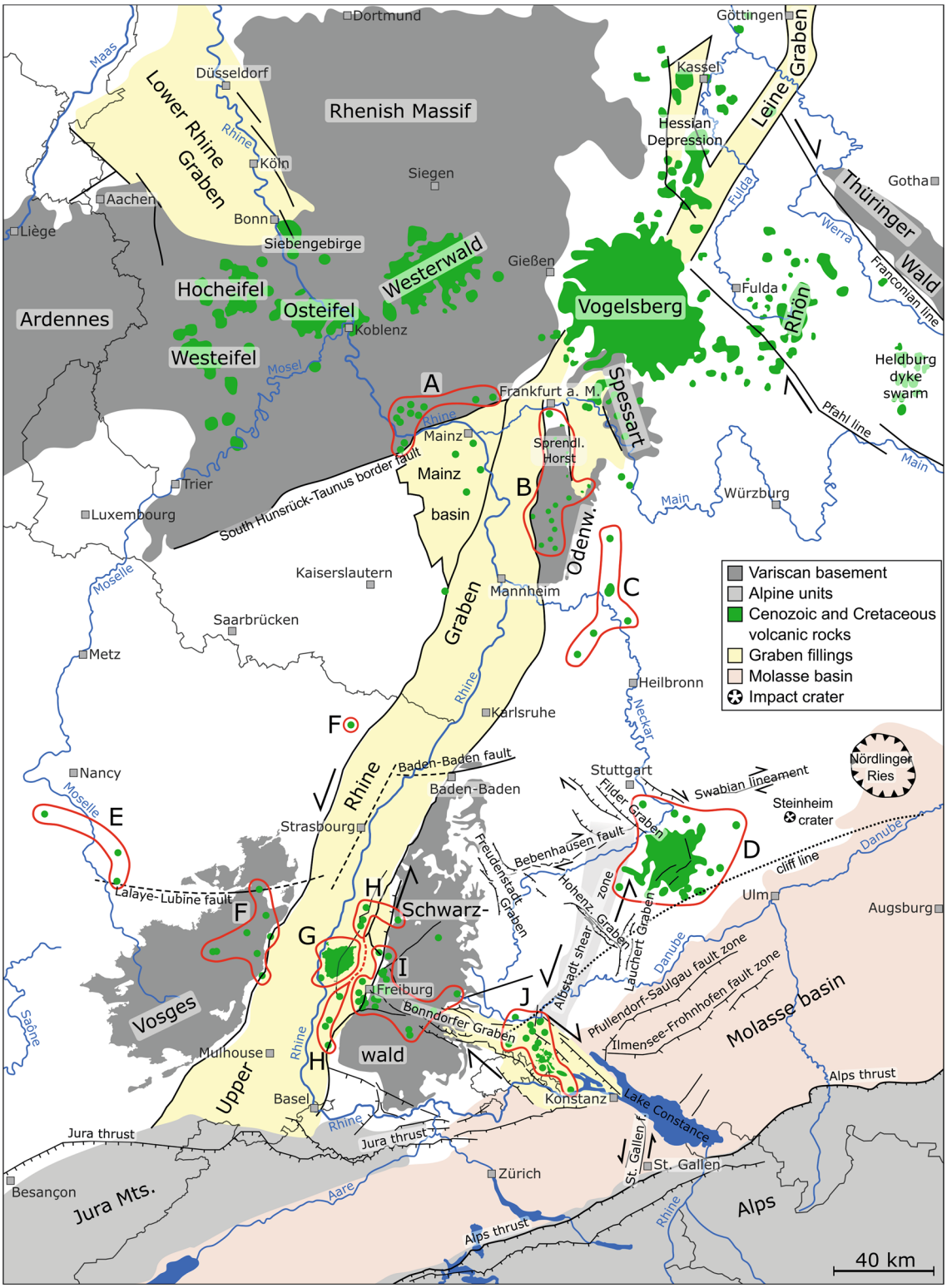

Fig. 4 Simplified geologic map of SW Germany and E France showing major tectonic structures, geological main units, and occurrences of late Cretaceous to Holocene volcanic rocks (modified after Egli et al. 2017; Ring and Bolhar 2020). *A* Taunus, *B* Lower Main plain, *C* Odenwald and Kraichgau area, *D* Urach, *E* Lorraine, *F* Vosges and Pfälzerwald, *G* Kaiserstuhl, *H* Southern Upper Rhine Graben, *I* Bonndorfer Graben and Freiburger Bucht area, *J* Hegau area

Lustrino and Wilson 2007; Wedepohl et al. 1994; Wedepohl and Baumann 1999; Wilson and Downes 1992; Wörner et al. 1986).

Petrogenetic models explaining the diversity of volcanic rocks in the CEVP

Previous studies from the Urach and Hegau areas suggested that melilititic rocks crystallized from very low-degree, volatile- and trace-element-rich partial melts that originated in the sub-lithospheric mantle (> 100 km depth; dolomite–garnet peridotite stability field) and infiltrated and metasomatized the overlying lithospheric mantle (~ 75 km; Dunworth and Wilson 1998), or in some cases directly erupted at the surface. Other models, however, locate the melt generation of melilite-bearing rocks in the CEVP at the base of the lithosphere (Blusztajn and Hegner 2002), possibly in the thermal boundary layer (TBL; Heldburg region; Pfänder et al. 2018). Despite the timing, origin, and processes of metasomatic overprint are not yet well constrained, previous modifications to ancient subduction processes are widely accepted as the major forces for metasomatic overprinting of the mantle (e.g., Blusztajn and Hegner 2002; Hegner and Vennemann 1997; Lustrino and Wilson 2007; Puziewicz et al. 2020; Ulrych et al. 2011; Witt-Eickschen and Kramm 1998). According to Pfänder et al. (2018), prolonged subduction of oceanic and continental lithosphere with successive dehydration during Variscan Orogeny generates aqueous to supercritical fluids enriched in volatiles and other trace elements, causing metasomatism at great depths (> 125 km) in the thickened lithosphere. This process results in the formation of a carbonated, phlogopite-bearing garnet lherzolite that is later partially melted during evolution of the ECRiS in response to perturbation of the TBL and decompression associated with lithospheric thinning (< 85 km). For instance, Hegner and Vennemann (1997) identified an influence of recycled seawater that overprinted the lithospheric mantle prior to melt formation at Urach and in the Hegau area. However, the asthenospheric mantle is often considered as another major melt source component in melilite-bearing rocks, interacting and mixing with lithospheric domains (Jung et al. 2006; Lustrino and Wilson 2007; Skála et al. 2015; Ulrych et al. 2008, 2013, 2016).

For melilite-free nephelinitic to basanitic rocks, slightly higher degrees of partial melting and shallower depths of extraction (spinel peridotite stability field or transition zone to garnet stability field) are assumed (Mertz et al. 2015; Pfänder et al. 2018; Schubert et al. 2015; Ulrych et al. 2013). Further, Ulrych et al. (2013) and Pfänder et al. (2018) suppose a less metasomatized lithospheric source for basanites than for the melilite-bearing rocks of the Heldburg region and the Eger Graben, without excluding an asthenospheric component. For basanites and nephelinites from the Westeifel, Vogelsberg, and Westerwald, Jung et al. (2011), Mertz et al. (2015), and Schubert et al. (2015) favor an asthenospheric source coupled with thermal erosion of strongly metasomatized lithosphere and/or intense asthenosphere–lithosphere interaction. The less primitive nature of some of these rocks was explained by temporary stagnation and early polybaric fractionation of olivine, clinopyroxene, and chromium spinel combined with contamination and mixing processes in the upper lithosphere, apparently consistent with frequent occurrence of resorbed green-core pyroxenes in the Westeifel and Hocheifel (Duda and Schmicke 1985; Jung et al. 2006).

Evolved phonolites from the Hegau have been suggested to represent differentiates of primitive foiditic magmas (Mahfoud and Beck 1989). Abratis et al. (2015) showed that (tephri)phonolites in the Heldburg dyke swarm were derived from a nephelinitic parental magma, but subsequently modified during stagnation and fractionation by mixing and mingling with basanitic melts, producing intermediate compositions. For trachytes and phonolites from the Rhön and the Lower Main Plain, assimilation of crustal rocks is suggested as another contribution to their formation (Jung et al. 2013; Schmitt 2006a).

In summary, some models for the CEVP invoke the involvement of mantle plumes or at least active diapiric upwelling (Dunworth and Wilson 1998; Haase et al. 2004; Hegner et al. 1995; Jung et al. 2006; Mertz et al. 2015; Schubert et al. 2015), whereas other studies doubt the necessity of mantle plumes and explain partial melting by earlier metasomatism in the mantle source (Blusztajn and Hegner 2002; Jung et al. 2005, 2011; Pfänder et al. 2018; Ulrych et al. 2008). Given the widely varying definitions of mantle plumes in terms of formation depth and thermodynamic properties, many of the modern models can be considered hybrid concepts. These do not attribute melting and volcanism exclusively to thermal or compositional anomalies of an uplifted asthenosphere, nor alone to metasomatism followed later by extensional–transtensional lithospheric thinning and uplift (Lustrino and Wilson 2007). However, deep-seated active asthenospheric upwelling causing a thermal anomaly below or in the TBL (mantle plumes in the narrower sense) is meanwhile mostly rejected for the formation of the CEVP (e.g., Fichtner and Villaseñor 2015).

Materials and methods

For this study, thin sections of 232 rock samples from approximately 130 localities in the CEVP were prepared for petrographic examination (Fig. 2), with a special focus on mineralogy, textures, and alteration state to classify them according to Le Maitre et al. (2002). Most samples originate

from various collections in Germany (University of Tübingen, Goethe University Frankfurt, University of Mainz, LGBR Freiburg, HLNUG Wiesbaden) and France (Terrae Genesis, Le Syndicat), supplemented by resampling of several localities. Based on the presence of datable minerals (perovskite, apatite, titanite, zircon, and/or pyrochlore) of adequate grain size, 56 thin sections from 45 localities were selected for U–Pb dating and supplemented by mounted heavy mineral concentrates from five localities (Online Resource 1).

U–Pb age data, supported by ~ 3000 spot analyses, were collected on a Thermo Scientific Element XR sector field ICP-MS coupled with a Resonetics RESOLution 193 nm ArF Excimer laser (CompexPro 102) at FIERCE (Goethe-Universität Frankfurt am Main) using a slightly modified method as previously described in Gerdes and Zeh (2006, 2009). The ICP-MS was tuned for maximum sensitivity while keeping the oxide formation (UO/U < 0.2%) and element fractionation (i.e., Th/U ~ 1) low. Analytical details are reported in the metadata tables of each sequence (Online Resource 2–13). Raw data were corrected offline using an in-house VBA Microsoft Excel© spreadsheet program (Gerdes and Zeh 2006, 2009). The $^{207}Pb/^{206}Pb$ and $^{206}Pb/^{238}U$ ratios were corrected for mass biases, including drift over time for each of the 11 sequences measured, using the primary reference material SRM-NIST 612. An additional correction was applied on the $^{206}Pb/^{238}U$ ratios to account for compositional differences using Durango apatite (31.44 Ma; McDowell et al. 2005), in-house Nama titanite (999 Ma; TIMS data, Wolfgang Dörr, pers. comm.), GJ-1 zircon (Jackson et al. 2004; 603 Ma; TIMS data, Wolfgang Dörr, pers. comm.), and Ice River perovskite (361 Ma; Tappe and Simonetti 2012). Ages were calculated using Isoplot 4.15 (Ludwig 2009) and are plotted within the Tera–Wasserburg space (Tera and Wasserburg 1972). All uncertainties are reported at the 2σ level and were calculated following the guidelines provided by Horstwood et al. (2016).

Results

Petrography

Based on mineralogy and textures, five groups of volcanic rock types that differ in spatial distribution are distinguished in the study area (Fig. 2): (1) olivine melilitites and melilite-bearing olivine nephelinites, (2) olivine nephelinites and nepheline basanites, (3) (phonolitic) haüynites and haüyne nephelinites, (4) phonolites, and (5) trachytes. Detailed information on the modal mineralogy of all rock types in the investigated regions is presented in Table 2, complemented by a TAS diagram (Fig. 3).

Olivine melilitites and melilite-bearing olivine nephelinites predominate at Urach, in the Hegau area, and in Lorraine and represent half of the occurrences in the southern URG but occur only rarely and often strongly altered in the Bonndorfer Graben and the Freiburger Bucht area and in the Vosges (Fig. 2). These are porphyritic rocks characterized by macrocrysts of melilite (< 2 mm; av. ~ 0.5 mm), olivine (< 10 mm; av. ~ 1 mm), and occasional clinopyroxene (< 2.5 mm; av. ~ 0.5 mm) set in a fine-grained groundmass of clinopyroxene, opaque phases, interstitial nepheline, melilite, biotite, betimes haüyne, and small amounts of subhedral to euhedral perovskite and apatite (Fig. 5a, b).

Olivine nephelinites and nepheline basanites, in contrast to the latter group, are melilite- and mostly perovskite-free. They are composed of macrocrysts of olivine (< 12 mm; av. ~ 1 mm) and clinopyroxene (< 10 mm; av. 1 mm) embedded in a very fine-grained or hyaline groundmass containing clinopyroxene, nepheline, and occasional haüyne. Such rocks are typical of the Vosges and Pfälzerwald, the Bonndorfer Graben and Freiburger Bucht area, the Taunus, the Lower Main plain, and parts of the Kaiserstuhl (Fig. 2). Two textural types of clinopyroxene macrocrysts can be distinguished: Type I is represented by beige to yellowish or pale brownish euhedral to subhedral crystals under polarized light. Type II (so-called green-core pyroxene, e.g., Duda and Schmincke 1985) consists of rounded greenish cores, surrounded by a fringe of Type I clinopyroxene. Some of these green-core pyroxenes enclose anhedral, stocky rounded apatite (Fig. 5c). Several samples with groundmass plagioclase and minor alkali feldspar are classified as basanitic nephelinites or nepheline basanites. Odenwald and Kraichgau samples may contain high amounts of biotite (Fig. 5d). In the Hegau area and the southern URG, some melilite-free olivine nephelinites occur as well (Fig. 2), but they lack green-core pyroxenes, contain betimes perovskite, and their texture is similar to the melilite-bearing rocks from these regions.

Haüynites to *phonolitic haüynites, and haüyne nephelinites to phonolitic haüyne nephelinites* are limited to few occurrences in the Odenwald and the Kraichgau area (Fig. 2). Medium-grained euhedral haüyne, Ti magnetite, and apatite phenocrysts surrounded by a fine-grained groundmass of nepheline, clinopyroxene, alkali feldspar, and amphibole are abundant. Subhedral poikiloblastic clinopyroxene macrocrysts (< 6 mm; av. 2 mm) form glomerules with inclusions of euhedral apatite and Ti magnetite crystals (Fig. 5e). Rare small subhedral olivine crystals are embedded in the groundmass. Further, evolved clinopyroxene-, nepheline-, and perovskite-bearing haüyne-melilititic to melilite-haüynitic dykes without any olivine occur in the Kaiserstuhl.

Phonolites in the eastern Hegau area are characterized by phenocrysts of alkali feldspar (< 5 mm; av. 1–2 mm), haüyne (< 3 mm; av. 0.5 mm), or their alteration products,

Table 2 Modal mineralogy of investigated rocks in the southern CEVP

Rock series/region	Ol	Cpx	Spl/Usp	Bt/Phl	Mll	Nph + Zeo	Hyn/Nsn/Sdl	Pl	Afs	Acc
Olivine melilitites and melilite-bearing nephelinites										
Hegau area	*20–40*	10–35	10–15	< 5	*< 20*	*< 20*	< 5	–	–	**prv,** ap
Urach	*20–50*	< 30	~ 15	< 5	*< 40*	*< 10*	< 5	–	–	**prv**, ap
Southern URG	*20–30*	25–30	< 20	< 5	*< 20*	*10–25*	Acc	–	–	**prv**, ap, grt
Lorraine	*25–35*	~ 30	10–15	Acc	*5–10*	*< 10*	Acc	–	–	**prv**
Vosges[a]	*~ 30*	~ 10	10–15	Acc	*15–20*	*< 5*	Acc	–	–	ap
Olivine nephelinites and nepheline basanites										
Vosges and Pfälzerwald	*20–30*	*40–55*	5–15	< 5	–	*5–20*	Acc	–	–	ap
Taunus	*10–35*	*35–50*	5–15	< 10	–	*< 20*	Acc	< 10	< 5	**ap**, ttn
Bonndorfer Graben and Freiburger Bucht	*10–40*	*20–60*	5–15	< 10	–	*< 20*	< 10	–	–	**ap**
Odenwald and Kraichgau area	*15–30*	*15–35*	10–20	*< 25*	–	*5–10*	< 5	< 15	< 5	ap
Lower Main plain	*20–25*	*30–35*	10–15	< 5	–	*20–25*	< 5	–	–	ap
Southern URG and Hegau area	*20–35*	*20–50*	10–15	< 5	–	*10–25*	Acc	–	–	**ap**, prv
(Phonolitic) haüynites and haüyne nephelinites										
Odenwald and Kraichgau area	< 10	*10–30*	15–20	< 10	–	< 10	*10–20*	–	< 10	***ap*** *(< 10)*
Kaiserstuhl[a]	–	5–20	5–10	< 5	*10–35*	5–10	*25–35*			***ap, prv****, grt*
Ijolites										
Hegau area[a]	–	*~ 30*	~ 10	Acc	–	*50–60*	–	–	–	**prv, ap**
Urach[a]	–	*~ 35*	~ 5	Acc	–	*~ 45*	–	–	–	**prv, ap**
Syenites and nepheline syenites										
Hegau area	–	*< 25*	Acc	< 5	–	*< 35*	–	–	*50–65*	**ttn, ap, zrn, pcl,** thn
Phonolites										
Hegau area	–	*10–20*	Acc	Acc	–	*15–30*	*15–25*	–	*40–50*	**ttn, ap,** zrn, pcl
Trachytes										
Lower Main plain	–	–	5–10	Acc	–	–	–	< 10	*85–95*	**zrn, ap,** ttn

Distinctive values are in italics, characteristic accessories are in bold

Ol olivine, *Cpx* clinopyroxene, *Spl* spinel group (including magnetite), *Usp* ulvöspinel, *Bt* biotite, *Phl* phlogopite, *Mll* melilite, *Nph* nepheline, *Zeo* zeolites, *Hyn* haüyne, *Nsn* nosean, *Sdl* sodalite, *Pl* plagioclase, *Afs* alkali feldspar, *Acc* accessory minerals, *ap* apatite, *prv* perovskite, *grt* garnet, *ttn* titanite, *zrn* zircon, *pcl* pyrochlore, *xtm* xenotime, *thn* thorianite

[a]The difference to 100% results from optically not resolvable mineral phases due to alteration or microcrystalline matrix minerals

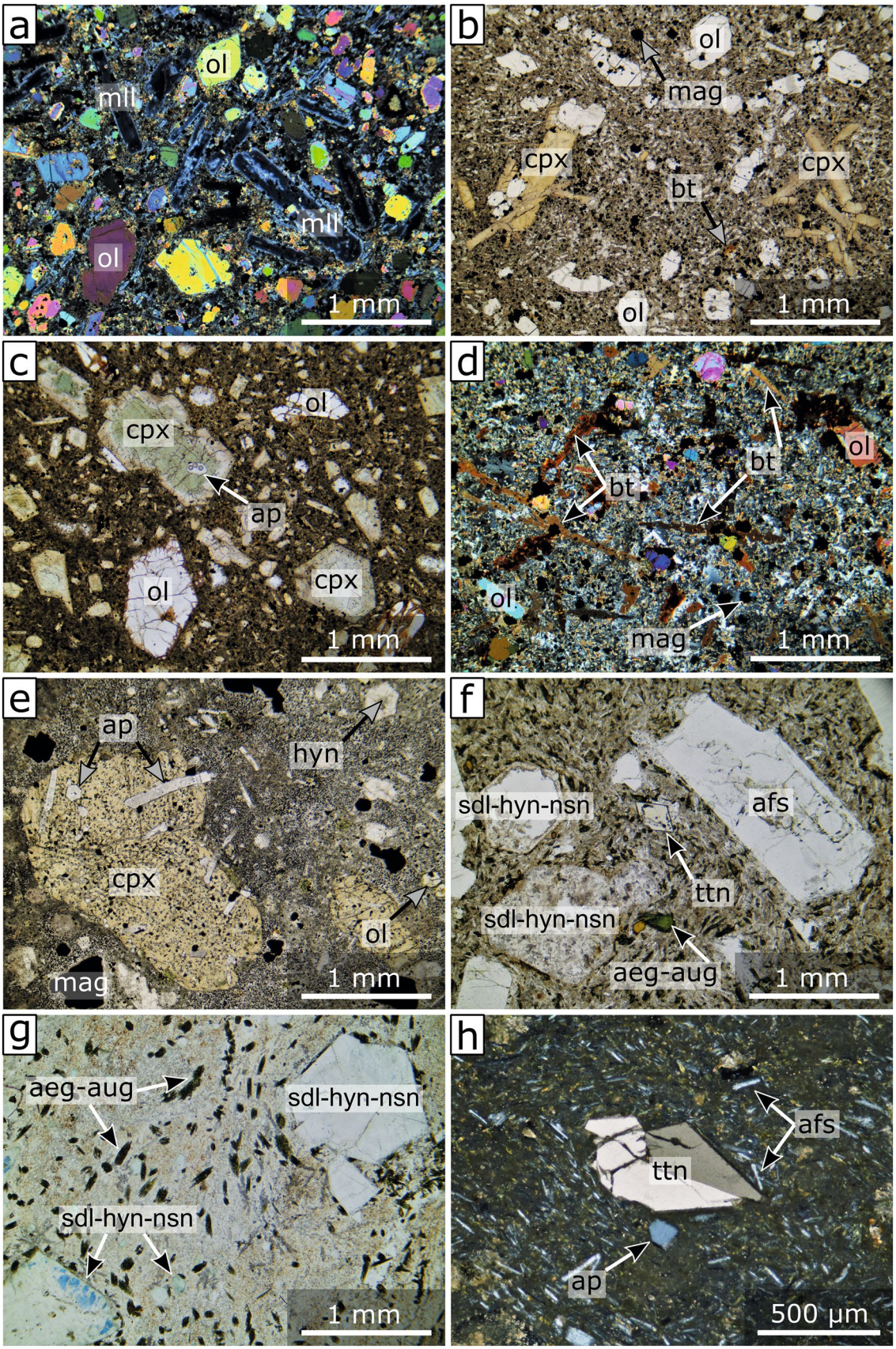
a
ol
mll
mll
ol
1 mm
b
ol
mag
cpx
cpx
bt
ol
1 mm
c
ol
cpx
ap
ol
cpx
1 mm
d
bt
bt
ol
ol
mag
1 mm
e
ap
hyn
cpx
ol
mag
1 mm
f
sdl-hyn-nsn
afs
ttn
sdl-hyn-nsn
aeg-aug
1 mm
g
aeg-aug
sdl-hyn-nsn
sdl-hyn-nsn
1 mm
h
afs
ttn
ap
500 µm

◂**Fig. 5** Microstructure and mineral textures in melilitites, foidites, basanites, and phonolites of the southern CEVP. **a** Olivine melilitite with olivine (ol) macrocrysts and melilite (mll) phenocrysts, crossed polarization (Hohenbol, Urach). **b** Nepheline-bearing olivine melilitite with olivine macrocrysts and agglomerations of clinopyroxene (cpx) in a groundmass of fine-grained clinopyroxene, melilite, nepheline, magnetite (mag), and little biotite (bt) (Hohenstoffeln, Hegau area). **c** Olivine nephelinite with olivine macrocrysts, clinopyroxene phenocrysts and resorbed green-core pyroxenes, containing an inclusion of anhedral apatite (ap), embedded in a cryptocrystalline groundmass (Rotteckruhe, Freiburger Bucht). **d** Phonolitic phlogopite-nepheline basanite with lath-shaped, large phlogopite and medium-grained olivine crystals in a groundmass of clinopyroxene, magnetite, nepheline, plagioclase, and minor alkali feldspar (Steinsberg, Kraichgau). **e** Olivine-bearing nepheline haüynite with poikiloblastic clinopyroxene enclosing euhedral apatite and haüyne (hyn), magnetite, and olivine phenocrysts in a groundmass of nepheline, clinopyroxene, and minor alkali feldspar (Neckarbischofsheim, Kraichgau). **f** Phonolite with phenocrysts of alkali feldspar (afs), a strongly altered sodalite group mineral (sdl–hyn–nsn), titanite (ttn) and aegirine-augite (aeg-aug) in a groundmass of alkali feldspar, aegirine-augite, and nepheline (Hohentwiel, Hegau area). **g** Phonolite with altered sodalite group minerals showing exsolution textures in a groundmass of aegirine-augite, alkali feldspar, nepheline, and sodalite group minerals (Hohenkrähen, Hegau area). **h** Phonolite with a phenocrystal of titanite and small apatite in a fine-grained groundmass of aegirine-augite, alkali feldspar, and nepheline (Hohentwiel, Hegau area)

and occasional aegirine-augite (< 1 mm) embedded in a groundmass of alkali feldspar, haüyne, nepheline, and aegirine–augite (Fig. 5f, g). Euhedral apatite, titanite, zircon, and rare pyrochlor are typical accessories (Fig. 5h). Some samples contain few biotite xenocrysts. *Trachytes* in the Lower Main plain (Hoher Berg near Heusenstamm and Sporneiche) consist of alkali feldspar phenocrysts (< 3 mm) and microcrysts along with minor amounts of opaque minerals, biotite, titanite, and zircon (Fig. 6a).

Additionally, two groups of coarse-grained magmatic rocks have been investigated: *ijolitic* veins and schlieren occur within the melilite-bearing rocks at Urach (Sternberg) and in the Hegau area (Hohenstoffeln). They are composed of euhedral, commonly sector-zoned, greenish clinopyroxene and subhedral, tabular nepheline and its alteration products, complemented by squat or skeletal, medium-grained Ti magnetite and euhedral apatite needles. Perovskite is abundant and forms either anhedral brownish grains (Urach, Fig. 6b) or purple skeletal crystals and crystal groups (Hegau area, Fig. 6c). *Syenitic to nepheline syenitic* fragments consisting of alkali feldspar, nepheline, and clinopyroxene, plus small amounts of biotite and opaque phases are enclosed in augite-hornblende-phlogopite tuffs, melilite-bearing olivine nephelinites, and phonolites from the Hegau area. Common accessory minerals are titanite, apatite, zircon (Fig. 6d), pyrochlore, and thorianite.

U–Pb geochronology

In situ U–Pb ages obtained on perovskite, apatite, titanite, zircon, and pyrochlore are listed and illustrated along with their 2σ errors, the number of measurement points (n), and the mean square weighted deviation (MSWD) in Tables 3 and 4 and in Fig. 7. The results reveal a late Cretaceous to early Eocene and a late Oligocene to late Miocene group separated by a ~ 20 Myr age gap. These age differences correlate with mineralogical differences and show systematic distribution patterns (Fig. 2): late Cretaceous to late Paleocene melilite-free olivine nephelinites and nepheline basanites occur in the Taunus (~ 68–55 Ma) and the Bonndorfer Graben and Freiburger Bucht area (~ 67–58 Ma), late Cretaceous to early Paleocene trachytes and haüynites are localized in the Lower Main plain (~ 73–65 Ma) and the Odenwald and Kraichgau area (~ 68–62 Ma). Late Oligocene to late Miocene perovskite-bearing olivine melilitites and melilite-bearing olivine nephelinites are restricted to Lorraine (~ 26 Ma), the southern URG (~ 26–25 Ma and 17–16 Ma), Urach (~ 19–12 Ma), and the Hegau area (12–9 Ma). Ages for ijolitic veins and schlieren therein (Hegau and Urach) are in good agreement with the host rock ages. Additionally, phonolites from five Hegau localities were dated to ~ 14–12 Ma and syenitic inclusions therein (Gönnersbohl) reveal ages of ~ 14–11 Ma. Nepheline syenitic xenoliths in tuffs and in melilite-bearing olivine nephelinites encompass a similar age range (~ 15–11 Ma), an augite-hornblende-phlogopite tuff yields ages of 14.5 ± 1.1 Ma and 12.5 ± 1.6 Ma, respectively. An exception from all these rock type–age relations is the polygenetic Kaiserstuhl, with melilite-rich rocks, melilite-free nephelinites, (phonolitic) tephrites/basanites, carbonatites, haüynites, phonolites, and noseanites, all of which erupted during the Miocene (~ 19–15 Ma; this study; Ghobadi et al. 2021).

Discussion

Timing and duration of volcanism in the southern CEVP

Using in situ U–Pb geochronology, we have dated numerous volcanic rocks of the southern CEVP for the first time, giving precise age constrains for several localities previously dated mostly by the K–Ar method on whole-rock samples (Baranyi et al. 1976; Horn et al. 1972; Kraml et al. 1995, 1999; Lippolt et al. 1963, 1973, 1975; Lippolt 1983). In comparison with previous literature data, the results of this dating approach, supplemented with published ages applying different modern methods, show two age groups in the southern CEVP (Figs. 7 and 8). Discrepancies and former uncertainties result from known problems of the K–Ar

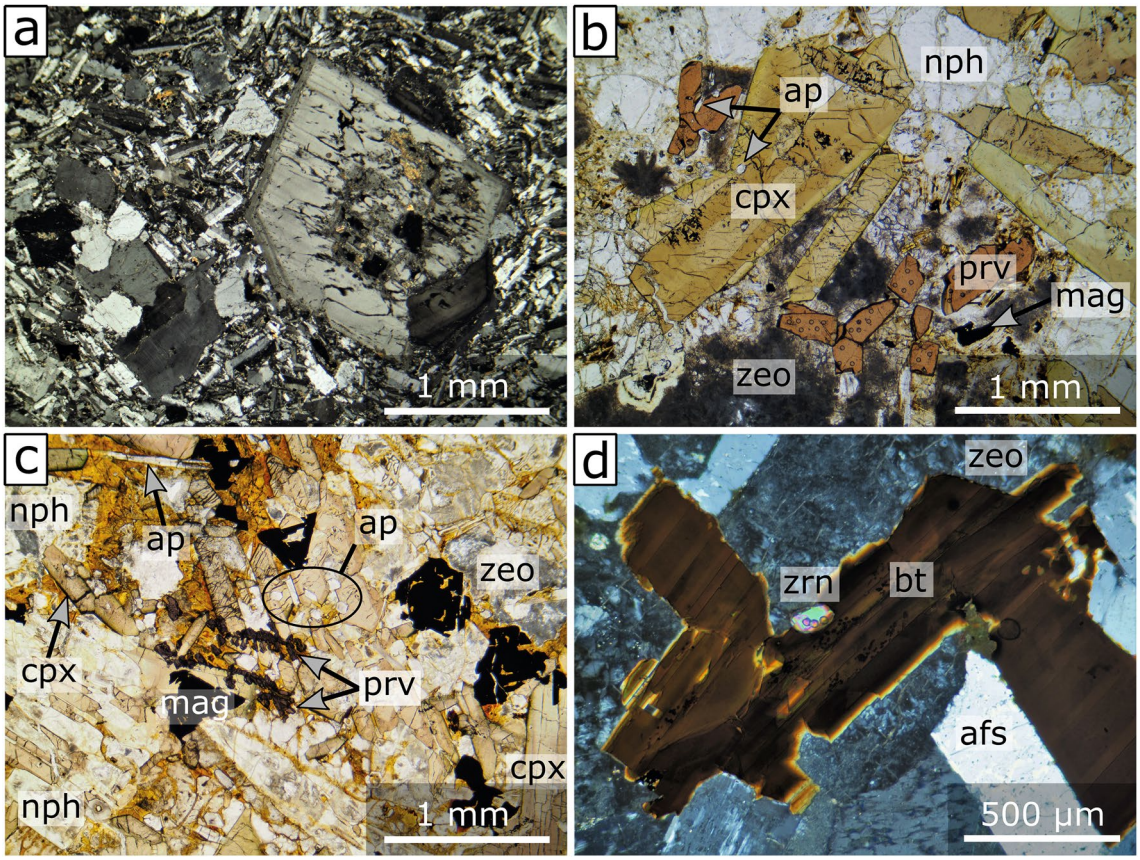

Fig. 6 Microstructure and mineral textures in trachytes, ijolites, and nepheline syenites of the southern CEVP. **a** Trachyte with a phenocryst of a sericitic altered, perthitic alkali feldspar and an accumulation of anhedral alkali feldspar in a groundmass of lath-shaped sanidine (Sporneiche, Lower Main plain). **b** Ijolite with euhedral sector-zoned clinopyroxene, tabular nepheline (nph), zeolite (zeo), and anhedral perovskite (prv) (Sternberg, Urach). **c** Ijolite with skeletal magnetite and perovskite surrounded by subhedral to euhedral clinopyroxene, nepheline, zeolite, and minor apatite (Hohenstoffeln, Hegau area). **d** Nepheline syenite xenolith with an anhedral zircon grain next to a tabular biotite crystal surrounded by alkali feldspar and zeolite (2 km E Weil, Hegau area)

method (e.g., Baranyi et al. 1976; Horn et al. 1972), such as loss of ^{40}Ar due to devitrification of rocks and alteration, particularly on small grains, or excess ^{40}Ar caused by inheritance during magma formation and/or ascent (e.g., wall rock contamination, presence of xenocrysts). Low closure temperatures for certain K-rich minerals and alteration-related K loss can also lead to erroneous age determinations. The old K–Ar ages are discussed in Online Resource 14.

Crystallization and cooling during ascent and emplacement of subvolcanic to volcanic rocks have no significant influence on the determined mineral ages, since 2σ uncertainties are generally larger than the duration of such processes (Schmitt 2006b; Schmitt et al. 2010; Sundermeyer et al. 2020). Thus, resolvable age differences between texturally distinct minerals in the same sample, between different samples of similar rock types from the same locality, and between plutonic cumulates and their volcanic host rocks allow for deciphering time spans of several Myr relevant for transcrustal plumbing systems at local and regional scales. Mineral ages in xenoliths may potentially suffer from thermal overprint by the host magma during ascent, which would result in partial reset of the original age if closure temperatures of the dated minerals are below those of the xenolith-transporting magma. Closure temperatures for the U–Pb system vary considerably between minerals, depending on grain size and cooling rate and increase from ~ 350–550 °C for apatite, via ~ 570–700 °C for titanite and ~ 660–950 °C for perovskite, to ~ 740–1010 °C for zircon (Carlson 2019; Chew and Spikings 2015; Flowers et al. 2007; Heaman and Parrish 1991; Spear and Parrish 1996; Wu et al. 2010). In the present study, several xenoliths of the same occurrence have been dated with different crystals and several different mineral phases (apatite, pyrochlore, titanite, zircon), with ages consistent within analytical uncertainty (Table 4). Thus, we consider them to represent crystallization ages of the xenoliths.

Our data (Tables 3 and 4) indicate that the oldest volcanic rocks in the southern CEVP formed in the late Cretaceous

Table 3 U–Pb ages of the late Cretaceous to early Eocene group

Sample	Locality	Rock type	Mineral	Age (Ma)	±2σ	*n*	MSWD
Taunus (A)							
75	Naurod (Erbsenacker)	ON	Ttn	55.38	0.91	34	0.91
75	Naurod (Erbsenacker)	ON	Ap	65.68	2.42	17	0.61
75-3	Naurod (Erbsenacker)	ON	Ap	68.13	2.41	32	0.96
Bonndorfer Graben and Freiburger Bucht area (I)							
N 119	Berghäuser Kapelle	Hyn b. ON	Ap	62.08	0.48	44	0.80
N 604	Berghäuser Kapelle	Hyn b. ON	Ap	59.13	2.22	27	1.09
N 604	Berghäuser Kapelle	Hyn b. ON	Zrn	59.55	1.35	18	1.79
N 251	Erentrudiskapelle Munzingen	Foiditic tuff	Ap	60.63	1.22	26	0.87
N 308	Heuweiler	Bt b. ON	Ap	66.54	2.92	11	1.16
N 46	Rautebacher Höfe	Hyn b. ON	Ap	62.81	0.87	57	1.21
N 104	Rotteckruhe	ON	Ap	59.86	0.96	11	0.62
N 96	St. Ottilien	Hyn, Bt b. ON	Ap	61.21	1.72	8	1.16
N 311	Tannengrund	ON	Ap	63.85	8.47	4	0.45
N 47	Uhlberg	Bt b. ON	Ap	64.57	1.18	12	1.10
Lower Main plain (B)							
HBH 1	Hoher Berg quarry near Heusenstamm	Trachyte	Ap	64.96	4.64	10	0.59
HBH 1	Hoher Berg quarry near Heusenstamm	Trachyte	Zrn	72.41	1.20	11	0.91
EPM 1	Sporneiche	Trachyte	Ap	66.83	6.43	18	0.59
GM 36	Sporneiche	Trachyte	Ap	68.51	6.27	18	0.89
GM 36	Sporneiche	Trachyte	Ttn	72.21	2.00	12	1.33
GM 36	Sporneiche	Trachyte	Zrn	72.60	1.46	6	0.79
Odenwald and Kraichgau area (C)							
N 595	Geisberg, Diedesheim	Bt b. NH	Ap	67.36	5.24	24	0.86
N 20	Hamberg near Neckarelz	Ol, Nph b. H	Ap	65.65	7.52	19	1.80
N 15	Neckarbischofsheim	ONH	Ap	67.71	8.65	54	0.63
I 20	Waldbrunn	Ol b. NH	Ap	62.32	4.27	52	0.94

b. bearing, *Bt* biotite, *Hyn* haüyne, *Nph* nepheline, *Ol* olivine, *NH* nepheline haüynite, *ON* olivine nephelinite, *ONH* olivine nepheline haüynite, *Ap* Apatite, *Ttn* titanite, *Zrn* zircon, *n* number of measurement spots, *MSWD* mean squared weighted deviation

and represent strongly evolved trachytes and haüyne-rich rocks from the Lower Main plain (~ 73–65 Ma) and the Odenwald and Kraichgau area (~ 70–62 Ma) in the east of the northern URG, consistent with U–Pb zircon ages in the same region for the Sporneiche trachyte (68.6 ± 1.9 Ma; Schmitt 2006a) and the Katzenbuckel phonolite (69.6 ± 1.9 Ma; Schmitt et al. 2007). A similar age range (~ 67–58 Ma) determined for the Freiburger Bucht and the Bonndorfer Graben area on the eastern flank of the URG coincides with the eruption of the Trois Épis olivine melilitite in the Vosges on the opposite graben shoulder with an amphibole $^{40}Ar/^{39}Ar$ age of 60.9 ± 0.6 Ma (Keller et al. 2002). For the Taunus, a new titanite age for Naurod (55.4 ± 0.9 Ma) is very similar to a $^{40}Ar/^{39}Ar$ age for Rabenkopf (58.7 ± 0.4 Ma; Fekiacova et al. 2007). However, significantly older ages for apatite inclusions in titanite (65.7 ± 2.4 Ma) and apatite in a second sample from Naurod (68.1 ± 2.4 Ma) reveal prolonged magmatic activity in this area started at least 10 Myr earlier, potentially revealing discontinuous magma replenishment events. During the early Eocene (~ 56–47 Ma), volcanism in the southern CEVP was basaltic to nephelinitic and restricted to the Lower Main plain and the Pfälzerwald (Forstberg, Messel maar, Stetteritz, Forst, and Kisselwörth; Fekiacova et al. 2007; Lenz et al. 2015; Lutz et al. 2013).

After a volcanic gap of ~ 20 Ma, the oldest known olivine melilitites of the younger series erupted in the late Oligocene (~ 26–25 Ma) near Essey-la-Côte in Lorraine and at the Buggingen potash salt deposit in the southern URG (Table 4). Subsequently, no magmatism is documented until a phase of intense volcanism represented at Urach (~ 19–12 Ma), in the Hegau area (~ 15–9 Ma), and the remaining southern URG (~ 17–16 Ma; Mahlberg, Herbolzheim) including the Kaiserstuhl volcanic complex (~ 19–15 Ma), whose activity is well constrained by recent dating of numerous rock types using U–Pb, $^{40}Ar/^{39}Ar$, Rb–Sr, (U-Th)/He, and fission track (Ghobadi et al. 2021 and references therein; Kraml et al. 1995, 1999), confirmed by our apatite and perovskite U–Pb ages for a haüyne melilitite from the Kaiserstuhl. The

Table 4 U–Pb ages of the late Oligocene to late Miocene group

Sample	Locality	Rock type	Mineral	Age (Ma)	±2σ	*n*	MSWD
Lorraine (E)							
LM 455	Essey-la-Côte	Nph b. OM	Prv	26.16	1.03	38	3.72
Southern URG (H)							
M 110	Buggingen	OM	Ap	24.68	1.80	41	1.23
M 110	Buggingen	OM	Prv	25.56	0.64	44	1.81
HERB	Herbolzheim	Foiditic tuff	Ap	16.75	0.84	120	1.00
2018-001	Mahlberg	ON	Prv	16.09	0.37	16	0.87
Kaiserstuhl (G)							
HTAC 1332	Horberig	HM	Ap	16.17	0.50	40	0.94
HTAC 1332	Horberig	HM	Prv	17.16	1.38	31	0.57
Urach (D)							
U 006	Am Hofwald	Bt b. OM	Prv	15.38	0.78	22	1.44
W 42	Autmuthbach	OM	Prv	12.30	1.09	14	1.64
U 028	Bölle	OM	Prv	13.29	4.56	25	2.16
U 018	Dietenbühl	Bt b. MON	Prv	13.53	1.38	27	0.90
M 10	Donnstetten	Nph b. OM	Prv	15.75	0.87	35	1.23
N 469	Eisenrüttel	Hyn b. ON	Prv	15.53	1.60	12	0.94
U 015	Eisenrüttel	Hyn b. ON	Prv	17.28	0.55	29	0.94
U 009	Floriansberg	Hyn b. OM	Prv	19.06	1.76	47	1.45
U 026	Floriansberg	Bt b. OM	Prv	14.18	0.36	10	0.90
U 005	Gaisbühl	OM	Prv	15.77	0.77	31	1.41
U 021	Götzenbrühl	Nph b. OM	Prv	14.66	1.18	35	0.89
833	Hohenbol near Owen	Nph b. OM	Prv	15.94	0.26	37	1.63
U 027	Hohenbol near Owen	OM	Prv	15.39	3.44	27	0.60
U 030	Hohenbol near Owen	Nph b. OM	Prv	15.49	2.64	27	0.58
U 031	Jusi	OM	Prv	18.90	2.70	13	1.29
U 032	Metzinger Weinberg	Nph b. OM	Prv	13.61	0.65	42	1.01
U 025	Schopfloch	OM	Prv	12.97	1.22	45	1.16
U 001	Sternberg	Ijolite	Ap	11.95	6.61	43	0.88
U 001	Sternberg	Ijolite	Prv	12.65	0.45	60	1.63
U 016	Sternberg	OM	Prv	13.95	2.32	21	0.82
U 022	Sulzburg	OM	Prv	14.02	1.68	27	0.67
U 010	Wittlinger Steige	OM	Prv	14.42	0.99	22	0.78
Hegau area (J)							
N 374	Blauer Stein (Steinröhren)	Mll b. ON	Prv	9.93	0.96	9	0.93
HEG 17	Hohenhewen	Mll b. ON	Prv	10.28	0.41	33	1.40
HEG 02	Hohenstoffeln	Ijolite	Prv	11.04	0.32	64	1.47
HEG 02	Hohenstoffeln	Ijolite	Ap	11.11	0.86	59	1.39
HEG 05	Hohenstoffeln	Ijolite	Prv	10.23	0.23	58	1.23
HEG 05	Hohenstoffeln	Ijolite	Ap	9.77	0.75	57	0.62
HEG 15	Neuhewen	Mll b. ON	Prv	11.67	0.38	34	1.15
GB-2	Gönnersbohl	Phonolite	Ap	12.83	0.95	29	0.71
GB-2	Gönnersbohl	Phonolite	Ttn	12.93	0.48	15	1.24
GB-2	Gönnersbohl	Syenite	Ap	11.85	1.95	30	0.83
GB-2	Gönnersbohl	Syenite	Ttn	11.60	1.35	28	1.18
2020-07	Gönnersbohl	Syenite	Ap	12.06	2.42	75	0.86
2020-07	Gönnersbohl	Syenite	Ttn	13.48	0.38	171	1.24
2020-07	Gönnersbohl	Syenite	Zrn	13.19	0.24	20	1.63
HK-2	Hohenkrähen	Phonolite	Ap	13.13	0.98	8	0.84
HK-2	Hohenkrähen	Phonolite	Ttn	12.77	0.32	25	1.17
HW 2a	Hohentwiel	Phonolite	Ap	12.70	0.65	30	0.85

Table 4 (continued)

Sample	Locality	Rock type	Mineral	Age (Ma)	±2σ	*n*	MSWD
HW 2a	Hohentwiel	Phonolite	Ttn	12.79	0.32	20	0.85
HW 2a	Hohentwiel	Phonolite	Zrn	12.91	0.21	24	0.90
MB-1	Mägdeberg	Phonolite	Ap	13.26	1.17	27	1.39
MB-1	Mägdeberg	Phonolite	Ttn	12.85	0.30	32	1.16
ST-1	Staufen	Phonolite	Ap	13.36	0.70	34	0.70
ST-1	Staufen	Phonolite	Ttn	12.35	0.30	31	1.41
HEG 09	Twiel SW, Elisabethenberg	Aug–Hbl–Phl tuff	Ap	12.49	1.57	47	1.18
H 7	Twiel SW, Elisabethenberg	Aug–Hbl–Phl tuff	Ap	14.51	1.11	30	1.13
HEG 06	Hohenstoffeln	NS	Ttn	13.56	0.46	43	0.80
HEG 06	Hohenstoffeln	NS	Zrn	14.43	1.20	7	0.38
N 248	2 km E Weil	NS	Pcl	11.79	0.34	31	1.54
N 248	2 km E Weil	NS	Zrn	12.85	0.32	16	1.62
E 403	2 km E Weil	NS	Pcl	12.42	0.32	26	0.84
E 403	2 km E Weil	NS	Zrn	12.90	0.24	44	1.70

b. bearing, *Aug* augite, *Bt* biotite, *Hbl* hornblende, *Hyn* haüyne, *Mll* melilite, *Nph* nepheline, *Ol* olivine, *Phl* phlogopite, *HM* haüyne melilitite, *MON* melilite olivine nephelinite, *NS* nepheline syenite, *OM* olivine melilitite, *ON* olivine nephelinite, *Ap* Apatite, *Pcl* pyrochlore, *Prv* perovskite, *Ttn* titanite, *Zrn* zircon, *n* number of measurement spots, *MSWD* mean squared weighted deviation

repeatedly stated hypothesis that volcanism at Urach was triggered by the Ries impact (e.g., Ring and Bolhar 2020) must be rejected, as several volcanic rocks (Table 4) and biostratigraphic evidence from Randeck maar sediments (14.8–17.0 Ma; Rasser et al. 2013) provide significantly older ages (Table 4) than the Ries impactites (e.g., $^{40}Ar/^{39}Ar$ age of 14.6 ± 0.2 Ma; Buchner et al. 2010). The igneous activity at Urach persisted ~ 7 Myr, significantly longer than the 2 Myr recently assumed by Kröchert et al. (2009) and Ring and Bolhar (2020). Towards the end of volcanism at Urach, relocation of magmatic activity from the northern to the southern tip of the Albstadt shear zone (Fig. 4) is expressed by phonolitic domes in the eastern Hegau (~ 14–11 Ma) and primitive melilititic to nephelinitic eruptions in the western Hegau (~ 12–9 Ma), representing the last magmatic signal in the southern CEVP. Age data from evolved nepheline syenitic xenoliths in tuffs and melilititic to nephelinitic rocks (~ 15–11 Ma) match those of the Hegau phonolites and syenitic autoliths therein. Thus, there is no age gap between the emplacement of primitive and evolved rocks, suggesting a close genetic relationship between both rock types and differentiation and storage processes over such time scales in the upper crust. The spatial separation of melilite-bearing nephelinites in the west and phonolites in the east may suggest that minor structural differences in the nature of the upper lithosphere led in some cases to prolonged stagnation and evolution in a magma chamber and in other cases to direct eruption. The ijolitic schlieren from the Hohenstoffeln are interpreted as in situ differentiation products accumulating and crystallizing from the surrounding magma, consistent with their identical age within the uncertainty compared to that of the nephelinitic host rock.

Chronological and petrographic relations within the CEVP

Compared to the northern part of the CEVP, where volcanic rocks are mostly represented by extensive polygenetic or diversely composed complexes and dyke swarms, those in the study area occur as small stocks, vents, or dykes either isolated (e.g., Taunus, Odenwald and Kraichgau area) or as larger fields (e.g., Urach, Hegau; Figs. 1 and 4, Table 1), with the Kaiserstuhl being a prominent exception. The northern volcanic rocks are only mildly SiO_2-undersaturated or SiO_2-saturated, forming basanitic to basaltic and more evolved rocks. Nevertheless, foidites and melilitites do occur as integral part of some volcanic regions in the northern CEVP such as Hessian Depression, Eifel, Rhön, Eger Graben, and Heldburg dyke swarm, too (Abratis et al. 2007, 2009, 2015; Büchner et al. 2015; Jung et al. 2006; Kramm and Wedepohl 1990; Mertz et al. 2015; Pfänder et al. 2018; Skála et al. 2015; Ulrych et al. 2016). Conversely, evolved rocks are rare in the study area, comprising phonolites in the eastern Hegau area, diverse Kaiserstuhl rocks, and trachytes in the Lower Main plain.

The age distribution for the northern and southern CEVP based on literature and our new data, disregarding K–Ar whole-rock ages (Fig. 8), indicates continuous volcanism since the middle Eocene at varying locations. In contrast to the southern part (Fig. 2), however, no obvious correlation between rock types and ages in the northern CEVP exists. The only evidence for late Cretaceous igneous activity in the northern CEVP are trachytic xenoliths and camptonitic dykes at the Vogelsberg, (~ 74–66 Ma; Bogaard and Wörner 2003; Martha et al. 2014; Schmitt et al. 2007). This

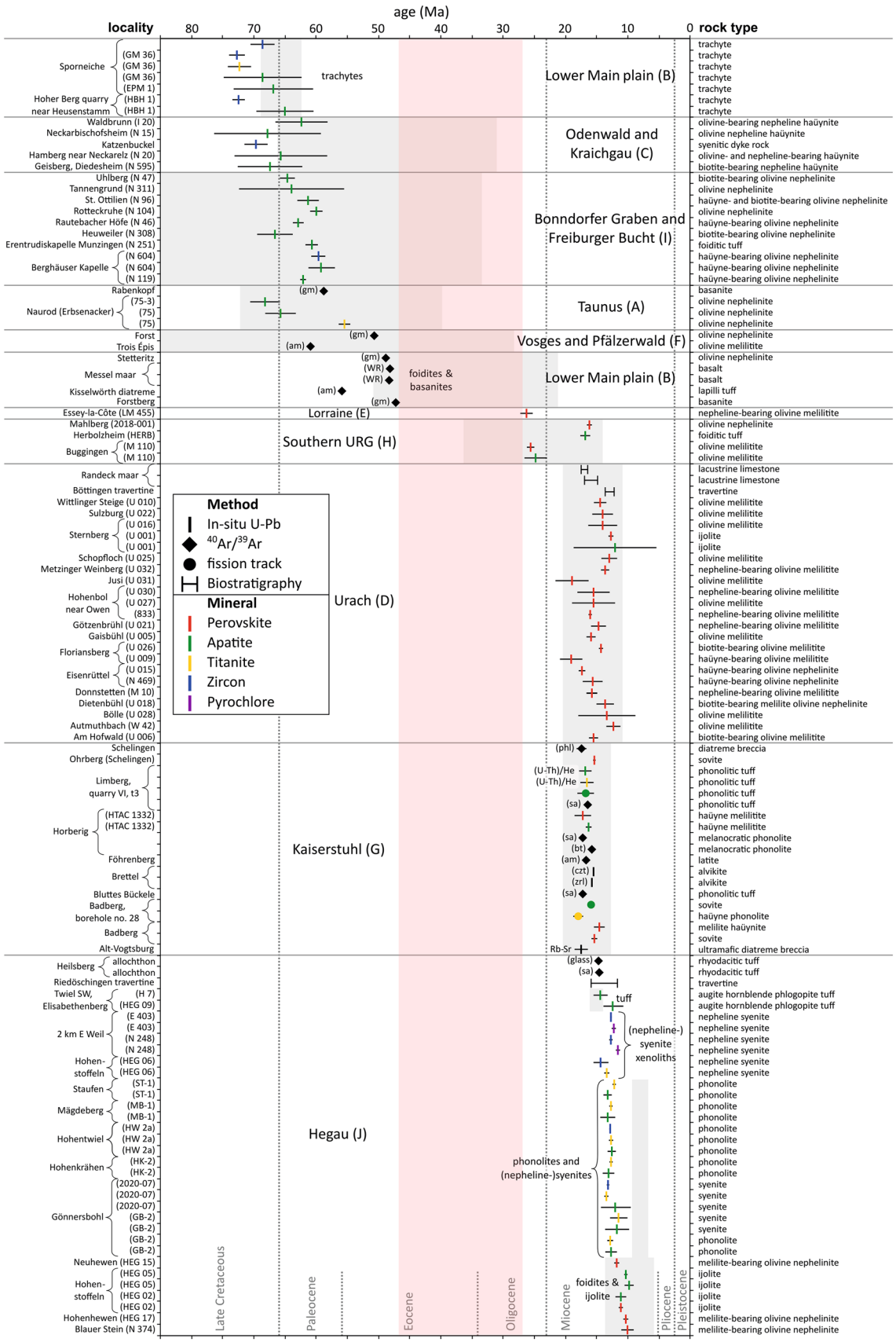
age (Ma)
80
70
60
50
40
30
20
10
0
locality
rock type
Sporneiche
(GM 36)
(GM 36)
(GM 36)
(EPM 1)
Hoher Berg quarry
(HBH 1)
near Heusenstamm
(HBH 1)
trachytes
Lower Main plain (B)
trachyte
trachyte
trachyte
trachyte
trachyte
trachyte
Waldbrunn (I 20)
Neckarbischofsheim (N 15)
Katzenbuckel
Hamberg near Neckarelz (N 20)
Geisberg, Diedesheim (N 595)
Odenwald and Kraichgau (C)
olivine-bearing nepheline haüynite
olivine nepheline haüynite
syenitic dyke rock
olivine- and nepheline-bearing haüynite
biotite-bearing nepheline haüynite
Uhlberg (N 47)
Tannengrund (N 311)
St. Ottilien (N 96)
Rotteckruhe (N 104)
Rautebacher Höfe (N 46)
Heuweiler (N 308)
Erentrudiskapelle Munzingen (N 251)
Berghäuser Kapelle
(N 604)
(N 604)
(N 119)
Bonndorfer Graben and Freiburger Bucht (I)
biotite-bearing olivine nephelinite
olivine nephelinite
haüyne- and biotite-bearing olivine nephelinite
olivine nephelinite
haüyne-bearing olivine nephelinite
biotite-bearing olivine nephelinite
foiditic tuff
haüyne-bearing olivine nephelinite
haüyne-bearing olivine nephelinite
haüyne-bearing olivine nephelinite
Rabenkopf
Naurod (Erbsenacker)
(75-3)
(75)
(75)
(gm)
Taunus (A)
basanite
olivine nephelinite
olivine nephelinite
olivine nephelinite
Forst
Trois Épis
(gm)
(am)
Vosges and Pfälzerwald (F)
olivine nephelinite
olivine melilitite
Stetteritz
Messel maar
Kisselwörth diatreme
Forstberg
(gm)
(WR)
(WR)
(am)
(gm)
foidites & basanites
Lower Main plain (B)
olivine nephelinite
basalt
basalt
lapilli tuff
basanite
Essey-la-Côte (LM 455)
Lorraine (E)
nepheline-bearing olivine melilitite
Mahlberg (2018-001)
Herbolzheim (HERB)
Buggingen
(M 110)
(M 110)
Southern URG (H)
olivine nephelinite
foiditic tuff
olivine melilitite
olivine melilitite
Randeck maar
Böttingen travertine
Wittlinger Steige (U 010)
Sulzburg (U 022)
Sternberg
(U 016)
(U 001)
(U 001)
Schopfloch (U 025)
Metzinger Weinberg (U 032)
Jusi (U 031)
Hohenbol near Owen
(U 030)
(U 027)
(833)
Götzenbrühl (U 021)
Gaisbühl (U 005)
Floriansberg
(U 026)
(U 009)
Eisenrüttel
(U 015)
(N 469)
Donnstetten (M 10)
Dietenbühl (U 018)
Bölle (U 028)
Autmuthbach (W 42)
Am Hofwald (U 006)
Urach (D)
lacustrine limestone
lacustrine limestone
travertine
olivine melilitite
olivine melilitite
olivine melilitite
ijolite
ijolite
olivine melilitite
nepheline-bearing olivine melilitite
olivine melilitite
nepheline-bearing olivine melilitite
olivine melilitite
nepheline-bearing olivine melilitite
nepheline-bearing olivine melilitite
olivine melilitite
biotite-bearing olivine melilitite
haüyne-bearing olivine melilitite
haüyne-bearing olivine nephelinite
haüyne-bearing olivine nephelinite
nepheline-bearing olivine melilitite
biotite-bearing melilite olivine nephelinite
olivine melilitite
olivine melilitite
biotite-bearing olivine melilitite
Method
In-situ U-Pb
40Ar/39Ar
fission track
Biostratigraphy
Mineral
Perovskite
Apatite
Titanite
Zircon
Pyrochlore
Schelingen
Ohrberg (Schelingen)
Limberg, quarry VI, t3
Horberg
(HTAC 1332)
(HTAC 1332)
Föhrenberg
Brettel
Bluttes Bückele
Badberg, borehole no. 28
Badberg
Alt-Vogtsburg
(phl)
(U-Th)/He
(U-Th)/He
(sa)
(sa)
(bt)
(am)
(czt)
(zrl)
(sa)
Rb-Sr
Kaiserstuhl (G)
diatreme breccia
sovite
phonolitic tuff
phonolitic tuff
phonolitic tuff
phonolitic tuff
haüyne melilitite
haüyne melilitite
melanocratic phonolite
melanocratic phonolite
latite
alvikite
alvikite
phonolitic tuff
sovite
haüyne phonolite
melilite haüynite
sovite
ultramafic diatreme breccia
Heilsberg
allochthon
allochthon
Riedöschingen travertine
Twiel SW, Elisabethenberg
(H 7)
(HEG 09)
2 km E Weil
(E 403)
(E 403)
(N 248)
(N 248)
Hohen-stoffeln
(HEG 06)
(HEG 06)
Staufen
(ST-1)
(ST-1)
Mägdeberg
(MB-1)
(MB-1)
Hohentwiel
(HW 2a)
(HW 2a)
(HW 2a)
Hohenkrähen
(HK-2)
(HK-2)
Gönnersbohl
(2020-07)
(2020-07)
(2020-07)
(GB-2)
(GB-2)
(GB-2)
(GB-2)
Neuhewen (HEG 15)
Hohen-stoffeln
(HEG 05)
(HEG 05)
(HEG 02)
(HEG 02)
Hohenhewen (HEG 17)
Blauer Stein (N 374)
Hegau (J)
(glass)
(sa)
tuff
(nepheline-) syenite xenoliths
phonolites and (nepheline-)syenites
foidites & ijolite
rhyodacitic tuff
rhyodacitic tuff
travertine
augite hornblende phlogopite tuff
augite hornblende phlogopite tuff
nepheline syenite
nepheline syenite
nepheline syenite
nepheline syenite
nepheline syenite
nepheline syenite
phonolite
phonolite
phonolite
phonolite
phonolite
phonolite
phonolite
phonolite
phonolite
syenite
syenite
syenite
syenite
syenite
phonolite
phonolite
melilite-bearing olivine nephelinite
ijolite
ijolite
ijolite
ijolite
melilite-bearing olivine nephelinite
melilite-bearing olivine nephelinite
Late Cretaceous
Paleocene
Eocene
Oligocene
Miocene
Pliocene
Pleistocene

◂**Fig. 7** Overview of all new in situ U–Pb age data amended by existing $^{40}Ar/^{39}Ar$, fission track, (U-Th)/He, Rb–Sr, and biostratigraphical results. The previous age distributions for the different regions based on old K–Ar age data are shown in light grey (Baranyi et al. 1976; Horn et al. 1972; Lippolt et al. 1963, 1973, 1975; Lippolt 1983). The current data indicates that there was no continuous primitive SiO_2-undersaturated volcanism in SW Germany and E France since the late Cretaceous, but two phases of activity separated by a middle Eocene to early Oligocene gap (shown in pink). This contrasts with previous K–Ar data. Age data from this work were supplemented with results from Aziz et al. (2010), Fekiacova et al. (2007), Ghobadi et al. (2021), Gregor (2003), Keller et al. (2002), Koban and Schweigert (1993), Kraml et al. (1995, 1999), Kraml et al. (2006), Lenz et al. (2015), Lutz et al. (2013), Rasser et al. (2013), Schleicher et al. (1990), Schmitt (2006a), Schmitt et al. (2007), and Wagner (1976). Note that for some $^{40}Ar/^{39}Ar$ and U–Pb ages, the published error range is smaller than the symbol size. *gm* groundmass, *WR* whole-rock, *am* amphibole, *phl* phlogopite, *sa* sanidine, *bt* biotite, *czt* calzirtite, *zrl* zirconolite

volcanic activity overlaps with the formation of trachytes in the Lower Main plain, haüyne-rich foidites in the Odenwald and Kraichgau area (Fig. 8), and an apatite inclusion age at Naurod (Taunus). The basaltic to nephelinitic rocks in the Lower Main plain and Pfälzerwald (~ 56–47 Ma) indicate the end of early magmatic activity in the southern CEVP.

In the Hocheifel region, basanites, basalts, and minor evolved rocks (latites, trachytes) erupted in the Eocene between ~ 45–35 Ma (Fekiacova et al. 2007; Mertz et al. 2000) and mark the beginning of Cenozoic magmatism in the northern CEVP. About 10 Myr later, trachytic tuffs were emplaced in the Osteifel (~ 25.5 Ma; Mertz et al. 2007). Subsequently, volcanic activity did not occur again in the Osteifel and in the Westeifel until the Quaternary (~ 760–10 ka; Mertz et al. 2015; Schmitt et al. 2017; Shaw et al. 2010; Singer et al. 2008; Sirocko et al. 2013; van den Bogaard 1995), producing both strongly SiO_2-undersaturated, primitive rocks such as basanites, tephrites, nephelinites, melilitites, and more evolved rocks like phonolite and trachytes, and minor carbonatites (Mertz et al. 2015; Schmitt et al. 2010; Sundermeyer et al. 2020; Wörner et al. 1986). Recurrent melilititic to nephelinitic volcanism formed parts of the Heldburg dyke swarm between ~ 38–25 Ma, complemented by basanites and a phonolite ~ 7 Myr later (~ 18–12 Ma; Abratis et al. 2007, 2015; Pfänder et al. 2018).

Basanites, alkaline basalts, and tholeiites formed throughout the Oligocene and the early Miocene in Lusatia (Eger Graben; ~ 35–27 Ma), the Siebengebirge (~ 31–22 Ma), the Westerwald (~ 25 Ma), the Rhön (24–18 Ma), and the Vogelsberg (~ 17–14 Ma), occasionally associated with latites, trachytes, and phonolites without a clear chronological sequence (Abratis et al. 2007; Bogaard et al. 2001; Büchner et al. 2015; Kolb et al. 2012; Linthout et al. 2009; Mayer et al. 2014; Mertz et al. 2007; Przybyla et al. 2018). Trachytic tuffs are also reported for the Wetterau in the northernmost Cenozoic successions of the URG (~ 26 Ma; Neuhaus 2010). Unlike the north, there is no evidence of volcanism in the southern CEVP for the middle Eocene to early Oligocene until sporadic eruptions of the second magmatic phase occurred ~ 26–25 Ma ago and were followed ~ 6 Myr later by recurrent, partly long-lasting volcanism at Urach, in the Kaiserstuhl, the southern URG, and the Hegau area (> 9 Ma), overlapping the Miocene activity of the Rhön, Vogelsberg, and Heldburg dyke swarm. In contrast to these regions, in the southern CEVP, mainly melilite-bearing nephelinites, melilitites, and subordinately basanites/tephrites, haüynites, phonolites, noseanites, and carbonatites (Kaiserstuhl, Hegau) were emplaced. The magmatic history coincides with increased hydrothermal activity around the URG (Walter et al. 2018) with U–Pb ages of hydrothermal carbonates indicating a late Cretaceous phase (~ 74–60 Ma) and a main Miocene to recent phase (< 20 Ma). However, increased hydrothermal activity from 40–28 Ma falls in a period of volcanic quiescence, and thus cannot be straightforwardly correlated with magmatism in the southern CEVP.

Pliocene volcanic rocks in Germany are only reported for the Westerwald, with a basanite dated to 5.0 ± 0.2 Ma (Schubert et al. 2015). Furthermore, a new phase of volcanic activity occurred in Lusatia in the Pleistocene (~ 370–170 ka; Mrlina et al. 2007; Wagner et al. 1998), coinciding with the Eifel volcanism. In the French Massif Central (~ 14 Ma–5 ka) and the Pannonian Basin (~ 18.5 Ma–8 ka), on the other hand, the main phase of volcanism dates back to the middle Miocene and has continued with short interruptions until today, the spectrum of erupted magmas ranging from basanites to rhyolites (Harangi et al. 2010, 2015; Hurai et al. 2013; Lexa et al. 2010; Lukács et al. 2018; Molnár et al. 2019; Nowell et al. 2006; Riisager et al. 2000; Seghedi and Downes 2011; Wijbrans et al. 2007).

Considering the entire CEVP, there are no obvious correlations between spatial, compositional, and temporal evolution of volcanism like propagating hot-spot tracks that would support a plume-like mantle anomaly (Lustrino and Wilson 2007). Although thermal asthenospheric upwelling cannot be ruled out as driving force, the most striking differences of the southern CEVP compared to the northern one, i.e., the ~ 20 Ma age gap, the more pronounced SiO_2-undersaturation of the rocks, and the usually monogenetic character, indicate a structural control on the occurrence of volcanism linked to the geodynamic evolution of Europe. However, there are some spatial variations at same times and temporal variations within same areas. For instance, in some regions with bimodal or polygenetic volcanism, primitive rocks follow more differentiated ones and/or strongly SiO_2-undersaturated rocks follow less SiO_2-undersaturated or SiO_2-saturated ones (e.g., Hegau, Vogelsberg; this study; Bogaard and Wörner 2003), sometimes vice versa (e.g., Heldburg; Abratis et al. 2015;

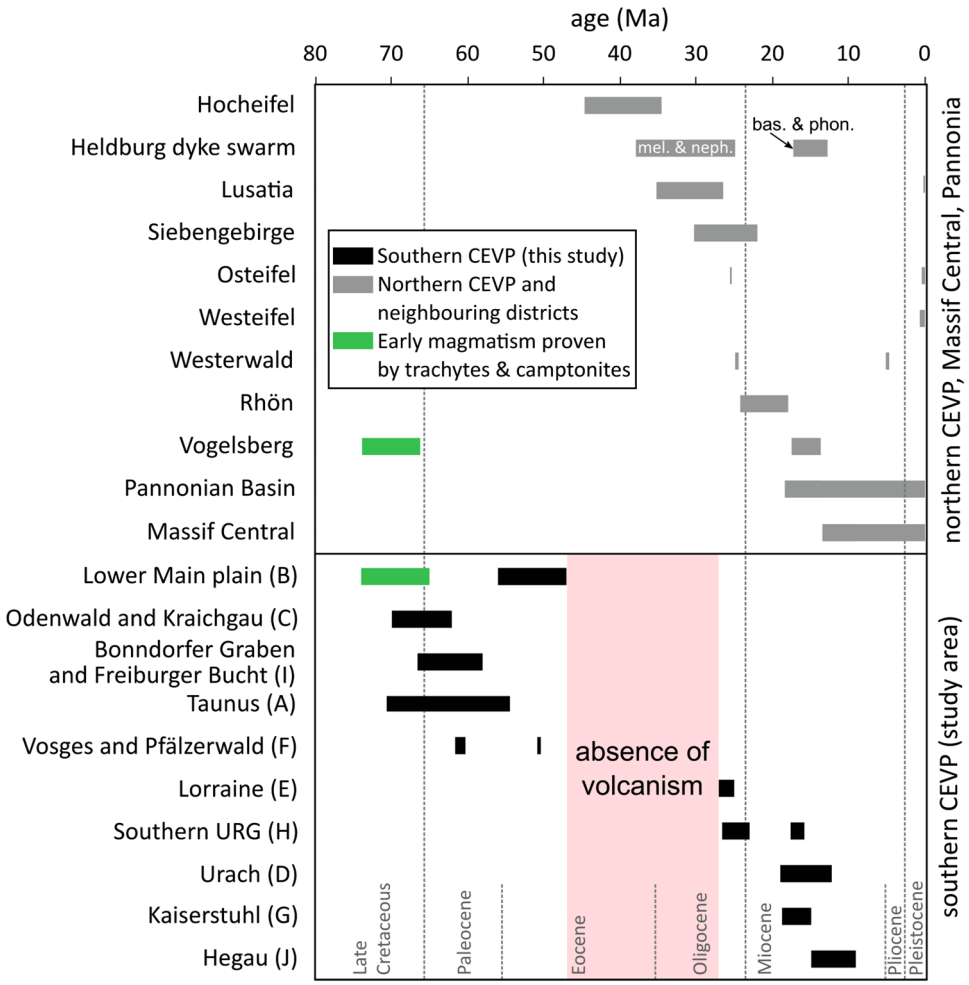

Fig. 8 Age distribution of igneous rocks in the Central European Volcanic Province. The data of this work are amended by literature data (except for K–Ar data; Abratis et al. 2007; Aziz et al. 2010; Büchner et al. 2015; Fekiacova et al. 2007; Ghobadi et al. 2021; Gregor 2003; Harangi et al. 2010; Harangi et al. 2015; Hurai et al. 2013; Keller et al. 2002; Koban and Schweigert 1993; Kraml et al. 1995, 1999; Kraml et al. 2006; Lenz et al. 2015; Lexa et al. 2010; Linthout et al. 2009; Lukács et al. 2018; Lutz et al. 2013; Mayer et al. 2014; Mertz et al. 2000; Mertz et al. 2007; Mertz et al. 2015; Molnár et al. 2019; Nowell et al. 2006; Pfänder et al. 2018; Przybyla et al. 2018; Rasser et al. 2013; Riisager et al. 2000; Schleicher et al. 1990; Schmitt 2006a; Schmitt et al. 2007; Schubert et al. 2015; Shaw et al. 2010; Singer et al. 2008; van den Bogaard 1995; Wagner 1976; Wagner et al. 1998; Wijbrans et al. 2007). Continuous magmatism throughout the province can be traced back to the late Cretaceous. However, primitive, strongly SiO_2-undersaturated volcanism in the southern CEVP is restricted to two periods: from the late Cretaceous to the early Eocene and from the late Oligocene to the late Miocene. *mel.* melilitites, *neph.* nephelinites, *bas.* basanites, *phon.* phonolites

Pfänder et al. 2018), and sometimes with age gaps as in the Eifel (Lustrino and Wilson 2007). In other regions, primitive rocks follow more differentiated ones, in turn succeeding primitive rocks (Büchner et al. 2015; Przybyla et al. 2018; Ulrych et al. 2011, 2013, 2016). Such compositional sequences have been attributed to pre-, syn-, and post-rift stages (e.g., Eger Graben; Ulrych et al. 2011), differentiation due to magmatic plumbing systems (e.g., Siebengebirge; Przybyla et al. 2018), and/or different sources and depths of melt generation (e.g., Heldburg region, Kaiserstuhl, Eger Graben; Braunger et al. 2018; Ghobadi et al. 2021; Pfänder et al. 2018; Ulrych et al. 2016). Likewise in the southern CEVP, the high temporal, spatial, and compositional variability of the individual regions on the one hand, and the compositional similarities of coeval occurrences on the other hand, refer to heterogeneities in the sub-lithospheric mantle beneath Central Europe (Puziewicz et al. 2020). The temporal trend for primitive rocks in the southern CEVP from melilite-free nephelinitic–basanitic rocks to melilite-bearing olivine nephelinites and olivine melilitites may indicate decreasing partial melting degrees, greater formation depths, a thicker lithosphere, a more carbonate-accentuated source, and/or a reduced influence of assimilation and fractional crystallization for the latter (e.g., Bogaard and Wörner

2003; Dunworth and Wilson 1998; Jung et al. 2006; Pfänder et al. 2018).

Implications for the geological evolution in the southern CEVP area

The older volcanic rocks of the southern CEVP (~ 73–47 Ma) postdate the late Cretaceous (~ 95–75 Ma) inversion tectonics in Central Europe (Voigt et al. 2021) and predate Upper Rhine Graben formation (< 47 Ma; Grimmer et al. 2017). Late Cretaceous to early Eocene volcanic activity in the southern CEVP overlaps in time with the ~ 75–55 Ma topographic uplift in Central Germany (Eynatten et al. 2021). The late Cretaceous inversion and the late Cretaceous to Eocene doming and respective magnitudes of shortening and uplift in the southern CEVP area are yet—due to the lack of Cretaceous sedimentary rocks—only inferred from apatite fission track and U–Th/He thermochronological data from the rift flanks of the URG (Link 2010). Time–temperature modeling of apatite fission track length distributions indicates late Cretaceous rapid cooling of crystalline basement rocks along both the western and eastern rift flanks of the URG (Link 2010), similarly to what documented in the Odenwald, Harz, and Thüringer Wald (Wagner et al. 1989; Eynatten et al. 2019, 2021; Thomson and Zeh 2000). A major portion of apatite fission track data in the Schwarzwald and Odenwald displays late Cretaceous to Eocene ages predating rift-related Cenozoic uplift and cooling (e.g., Link 2010; Wagner et al. 1989). A well-defined erosional angular unconformity recording a > 100 Myr hiatus in the subcrop of the URG documents this pre-Eocene uplift and erosion (e.g., Grimmer et al., 2017). In the northern URG, removal of the entire Mesozoic succession indicates that a zone of major uplift was probably located in the Taunus–Odenwald area, where numerous late Cretaceous to early Eocene volcanic rocks are documented as well. The dynamic topography concept of Eynatten et al. (2021) considers that thermally induced uplift of the lithosphere–asthenosphere boundary (LAB) and regional-scale doming terminated the late Cretaceous inversion at ~ 75 Ma in Central Germany. On the other hand, SW–NE shortening was probably ongoing until ~ 42 Ma along the western European continental margin (> 1000 km to the NW in Ireland), as indicated by calcite twinning analysis (Craddock et al. 2022). Eynatten et al. (2021) suggest that late Cretaceous to Eocene LAB uplift caused a dynamic topography of ~ 1 km and concomitant erosion of up to ~ 4 km. The formation of low-percentage melts that translocated to upper crustal levels appears to be controlled by interfering processes such as LAB shallowing and decompression, metasomatism, and deep-rooted faults such as the URG boundary fault system and the Albstadt shear zone. Dynamic topography can be induced by either convection-induced LAB uplift and subsequent cooling (or an abatement of LAB shallowing) or by translocation of continental lithosphere over upward convecting asthenospheric domains (e.g., Braun et al. 2013). Domal uplift terminated late Cretaceous shortening at ~ 75 Ma in western Central Europe. Late Cretaceous to early Eocene volcanic rocks occur around and possibly in the subcrop of the northern URG, where major uplift is considered for the Odenwald and southern Taunus, but also in the southern Schwarzwald (Bonndorfer Graben and Freiburger Bucht; Figs. 1 and 8; Table 3). Dykes strike NW, N, and NE as documented from maps, geophysical anomalies, and field observations (e.g., Mäussnest 1975; Stellrecht and Emmermann 1970). The ~ 47–27 Ma volcanic age gap temporarily overlaps with the early Eocene to Oligocene syn-rift phase of the URG during (W)NW-extension (e.g., Schumacher 2002).

A major change in deformation characterized by (E)NE-trending extension and transtension is considered to have started ~ 18 Ma (Schumacher 2002) or earlier (~ 25 Ma; Grimmer et al. 2017), associated with major activity of the NNW-trending Ludwigshafen hinge zone and the onset of distinct early Miocene subsidence of the Heidelberg basin (e.g., Grimmer et al. 2017). U–Pb ages of calcite fibers from NNE-trending Alpenrhein graben boundary faults yield 25.3 ± 5.6 Ma to 21.8 ± 3.4 Ma, interpreted with the initial phase of graben formation postdating Helvetic nappe emplacement (Ring and Gerdes 2016). The NNE-trending phonolitic Heldburg dyke (Fig. 1), yielding 17–14 Ma ($^{40}Ar/^{39}Ar$-ages; Abratis et al. 2015), and U–Pb ages of NW-striking calcite veins of 15.3–2.3 Ma from Miocene domal uplift (Ring and Bolhar 2020) indicate that (E)NE-extension was initiated at that time and persisted during Miocene domal uplift, volcanism, and erosion, and hence throughout the Neogene. Apparent conformable sedimentation in the URG from ~ 47 Ma to ~ 18–16 Ma was interrupted by uplift and erosion, resulting in a rift-wide, angular unconformity that separates conformably deposited older graben filling sediments in the footwall from younger, i.e., Pliocene to Quaternary graben fillings (e.g., Grimm 2011). The late Oligocene to late Miocene volcanic activity (~ 27–9 Ma; Table 4) temporarily overlaps with middle to late Miocene domal uplift in the southern CEVP as documented by the Burdigalian cliff (~ 20–18 Ma) elevated to > 900 m a.s.l. in the WSW and to < 400 m a.s.l. in the ENE of the Swabian Alb (Hoffmann 2017; Fig. 4), and by Miocene apatite fission track data in the southern Schwarzwald (Timar-Geng et al. 2006). East of the southern Schwarzwald, the Upper Miocene younger Juranagelfluh in the Hegau area comprises a late Miocene unroofing sequence, documenting erosion of an uplifted area in the W to NW of the Hegau area (Schreiner 1965). Dykes and elongated plugs show variable trends in the Hegau and Urach areas (e.g., Mäussnest 1974), indicating that pre-existing, shallow-rooted structures were used for the emplacement of melts, either locally along pre-existing

structures or during variations between strike-slip and normal faulting in the northern foreland of the Alps (Egli et al. 2017; Grimmer et al. 2017; Ring & Bolhar 2020; Craddock et al. 2022). In summary, though several details and processes still need to be clarified and quantified, it appears that since ~ 75–70 Ma dynamic topography has exerted major control on deformation, structural, and sedimentological development of the URG area and correlates temporally with the volcanic activity in the southern CEVP until today.

Conclusion

Based on new U–Pb mineral ages (perovskite, apatite, titanite, zircon, pyrochlor) for volcanic rocks and related plutonic inclusions from nine regions in the southern CEVP and complemented by existing age data, two distinct periods of volcanism are identified, with an age gap of ~ 20 Ma in between: a late Cretaceous to early Eocene (~ 73–47 Ma) group and a late Oligocene to late Miocene (~ 27–9 Ma) group. These two groups also differ in terms of mineralogy and spatial distribution coinciding with topographically uplifted areas. The older group occurs in the Lower Main plain, the Odenwald and Kraichgau area, the Taunus, the Bonndorfer Graben and Freiburger Bucht area, the Vosges and the Pfälzerwald and mostly comprises nephelinites, basanites, haüynites, and trachytes. The young group is mainly represented by perovskite-bearing olivine melilitites, melilite-bearing olivine nephelinites, and phonolites of Lorraine, the southern URG, Urach, and the Hegau area. As an exception, the Kaiserstuhl comprises basanites, tephrites, melilitites, nephelinites, haüynites, carbonatites, phonolites, and noseanites, all of which are of Miocene age.

Magmatism in both periods is linked to dynamic topography and the tectonic evolution in Central Europe, expressed in its age and location, reflecting large-scale stress field changes in the interplay of Pyrenean and Alpine orogeny interrupted by phases of subsidence causing a volcanic hiatus. The older volcanic rocks tend to occur in or along NE–SW striking structures and/or in the periphery of or on the shoulders of present-day graben structures (Fig. 4). They postdate late Cretaceous inversion tectonics (NE shortening; > 73 Ma) and, together with erosion of Permo-Mesozoic units, possibly reflect late Cretaceous to Eocene doming, shortening and uplift in the southern CEVP. The temporal and spatial coincidence of the 47–27 Ma volcanic gap with the initial phase of the URG development suggests a lithosphere-scale event such as cooling-induced regional subsidence and/or an abatement of asthenospheric uplift following the 75–55 Ma period considered for dynamic topography in Central Germany. The younger volcanic rocks are bound to Cenozoic N–S striking fault zones that developed with the ongoing formation of the ECRiS during Neogene (E) NE-extension–transtension (< 25 Ma). Again, this partly coincides with doming, uplift, and erosion in the southern CEVP and the URG from the middle to late Miocene, followed by subsidence during the Pliocene and Quaternary.

Evolved phonolites and (nepheline) syenite xenoliths in the melilite-bearing nephelinites of the Hegau area show that felsic alkaline magmatism beneath the Hegau area was already active before ~ 15 Ma, predating the first melilititic to nephelinitic eruptions (~ 12 Ma ago). The onset of volcanism is possibly related to the simultaneous attenuation, extinction, and relocation of Urach volcanic activity (19–12 Ma) at the northern tip of the Albstadt shear zone. Volcanism at Urach was not caused by the Ries impact (14.6 ± 0.2 Ma).

Magmatism in the northern part of the CEVP differs from the igneous activity in the southern sectors studied here. The generally mildly SiO_2-undersaturated volcanic rocks of the northern CEVP cover larger areas mostly forming voluminous, diversely composed complexes and are often more evolved than the isolated and low-volume, primitive nephelinites and melilitites in the southern CEVP. Even though volcanism in the northern CEVP has been recurrently active since the middle Eocene and the 20 Myr gap is absent, some temporal parallels with activity in the southern CEVP are apparent. Altogether, a spatial heterogeneous sub-lithospheric mantle source, varying lithospheric and crustal thicknesses, different depths of melt formation and degrees of partial melting, differentiation processes, and crustal contamination combined with the tectonic evolution in Central Europe can explain the different compositions of volcanic rocks and the magmatic evolution in the CEVP. The petrography and new age data do not provide evidence for a large-scale and deep-routed active asthenospheric upwelling beneath Central Europe. However, to delimit, determine, and describe these possible causes more precisely, detailed geochemical and petrological studies are in progress.

Supplementary Information The online version contains supplementary material available at https://doi.org/10.1007/s00531-022-02278-y.

Acknowledgements We thank Simone Schafflick, Philip Werner, and Alexander Rettenberger for sample preparation (University of Tübingen). We also thank Horst Marschall and Peter Prinz-Grimm (Goethe University Frankfurt) as well as Udo Neumann (University of Tübingen), D. Nesbor, L. Behr (HLNUG) and Kirsten Grimm (University of Mainz) for providing samples used in this study. We would especially like to thank Cyrille Delange and Luc Jaillard (Terrae Genesis) and Klaus Brauch (terratec Geophysical Services), who contributed with sampling in the field for us. Constructive comments by Dr. Jörg A. Pfänder, an anonymous reviewer, and the Editor-in-Chief Dr. Ulrich Riller greatly improved the manuscript and are gratefully acknowledged. FIERCE would like to acknowledge the financial support by the Wilhelm and Else Heraeus Foundation and the Deutsche Forschungsgemeinschaft (DFG). This is FIERCE contribution No. 117.

Author contributions Writing—original draft: TB, JG, AB. Writing—review and editing: MAWM, GM, TB, BFW, JG, TW. Visualization: TB. Investigation: TB, AG, AB, TW. Formal analysis: AB, AG, TB,

TW. Validation: AG. Conceptualization: MAWM, GM, TB. Project administration: GM, MAWM. Resources: GM, AG. Funding acquisition: MAWM, BFW, GM. Supervision: GM.

Funding Open Access funding enabled and organized by Projekt DEAL. This work was funded by the Deutsche Forschungsgemeinschaft (DFG)—Grant MA 2563/19 and WA 3116/6.

Data availability All research data are provided in Supplemental Information of the online version.

Declarations

Conflict of interest The authors declare that they have no known competing financial interests or personal relationships that could have appeared to influence the work reported in this paper.

References

Abratis M, Mädler J, Hautmann S, Leyk H-J, Meyer R, Lippolt HJ, Viereck-Götte L (2007) Two distinct Miocene age ranges of basaltic rocks from the Rhön and Heldburg areas (Germany) based on $^{40}Ar/^{39}Ar$ step heating data. Geochemistry 67(2):133–150. https://doi.org/10.1016/j.chemer.2006.03.003

Abratis M, Munsel D, Viereck-Götte L (2009) Melilithite und Melilithführende Magmatite des sächsischen Vogtlands: petrographie und Mineralchemie. Z Geol Wiss 37(1–2):41–79

Abratis M, Viereck L, Pfänder JA, Hentschel R (2015) Geochemical composition, petrography and $^{40}Ar/^{39}Ar$ age of the Heldburg phonolite: implications on magma mixing and mingling. Int J Earth Sci (geol Rundsch) 104(8):2033–2055. https://doi.org/10.1007/s00531-015-1207-x

Albers M, Christensen UR (1996) The excess temperature of plumes rising from the core-mantle boundary. Geophys Res Lett 23(24):3567–3570. https://doi.org/10.1029/96GL03311

Aziz HA, Böhme M, Rocholl A, Prieto J, Wijbrans JR, Bachtadse V, Ulbig A (2010) Integrated stratigraphy and $^{40}Ar/^{39}Ar$ chronology of the early to middle Miocene Upper Freshwater Molasse in western Bavaria (Germany). Int J Earth Sci (geol Rundsch) 99(8):1859–1886. https://doi.org/10.1007/s00531-009-0475-8

Baranyi I, Lippolt HJ, Todt W (1976) Kalium-Argon-Altersbestimmungen an tertiären Vulkaniten des Oberrheingraben-Gebietes: II Die Alterstraverse vom Hegau nach Lothringen. Oberrh Geol Abh 25(1):41–62

Blusztajn J, Hegner E (2002) Osmium isotopic systematics of melilitites from the Tertiary Central European Volcanic Province in SW Germany. Chem Geol 189(1–2):91–103. https://doi.org/10.1016/S0009-2541(02)00143-2

Bogaard PJF, Wörner G, Henjes-Kunst F (2001) Chemical stratigraphy and origin of volcanic rocks from the drill-core "Forschungsbohrung Vogelsberg 1996". In: Hoppe A, Schulz R (eds) Die Forschungsbohrung Vogelsberg 1996. Einblicke in einen miozänen Vulkankomplex, vol 107, Wiesbaden, pp 69–99

Bogaard PJF, Wörner G (2003) Petrogenesis of Basanitic to Tholeiititic Volcanic Rocks from the Miocene Vogelsberg. Central Germany J Petrol 44(3):569–602. https://doi.org/10.1093/petrology/44.3.569

Braun J, Robert X, Simon-Labric T (2013) Eroding dynamic topography. Geophys Res Lett 40(8):1494–1499. https://doi.org/10.1002/grl.50310

Braunger S, Marks MAW, Walter BF, Neubauer R, Reich R, Wenzel T, Parsapoor A, Markl G (2018) The Petrology of the Kaiserstuhl Volcanic Complex, SW Germany: the Importance of Metasomatized and Oxidized Lithospheric Mantle for Carbonatite Generation. J Petrol 59(9):1731–1762. https://doi.org/10.1093/petrology/egy078

Buchner E, Schwarz WH, Schmieder M, Trieloff M (2010) Establishing a 14.6 ± 0.2 Ma age for the Nördlinger Ries impact (Germany)—a prime example for concordant isotopic ages from various dating materials. Meteorit Planet Sci 45(4):662–674. https://doi.org/10.1111/j.1945-5100.2010.01046.x

Büchner J, Tietz O, Viereck L, Suhr P, Abratis M (2015) Volcanology, geochemistry and age of the Lausitz Volcanic Field. Int J Earth Sci (geol Rundsch) 104(8):2057–2083. https://doi.org/10.1007/s00531-015-1165-3

Carlson RW (2019) Absolute age determinations: radiometric. In: Gupta HK (eds) Encyclopedia of solid earth geophysics. Encyclopedia of Earth Sciences Series. Springer, Cham, pp 1–8. https://doi.org/10.1007/978-3-030-10475-7_69-1

Chew DM, Spikings RA (2015) Geochronology and thermochronology using apatite: time and temperature, lower crust to surface. Elements 11(3):189–194. https://doi.org/10.2113/gselements.11.3.189

Craddock JP, Ring U, Pfiffner OA (2022) Deformation of the European Plate (58–0 Ma): evidence from Calcite Twinning Strains. Geosciences 12(6):254. https://doi.org/10.3390/geosciences12060254

Dahl PS (1997) A crystal-chemical basis for Pb retention and fission-track annealing systematics in U-bearing minerals, with implications for geochronology. Earth Planet Sci Lett 150(3–4):277–290. https://doi.org/10.1016/S0012-821X(97)00108-8

Dèzes P, Schmid SM, Ziegler PA (2004) Evolution of the European Cenozoic Rift System: interaction of the Alpine and Pyrenean orogens with their foreland lithosphere. Tectonophysics 389(1–2):1–33. https://doi.org/10.1016/j.tecto.2004.06.011

Duda A, Schmincke H-U (1985) Polybaric differentiation of alkali basaltic magmas: evidence from green-core clinopyroxenes (Eifel, FRG). Contrib Mineral Petrol 91(4):340–353. https://doi.org/10.1007/BF00374690

Dunworth EA, Wilson M (1998) Olivine Melilitites of the SW German Tertiary Volcanic Province: mineralogy and Petrogenesis. J Petrol 39(10):1805–1836. https://doi.org/10.1093/petroj/39.10.1805

Egli D, Mosar J, Ibele T, Madritsch H (2017) The role of precursory structures on Tertiary deformation in the Black Forest—Hegau region. Int J Earth Sci (geol Rundsch) 106(7):2297–2318. https://doi.org/10.1007/s00531-016-1427-8

Fekiacova Z, Mertz DF, Renne P (2007) Geodynamic Setting of the Tertiary Hocheifel Volcanism (Germany), Part I: $^{40}Ar/^{39}Ar$ geochronology. In: Ritter JR, Christensen UR (eds) Mantle Plumes A Multidisciplinary Approach, 1st edn. Springer, Berlin, pp 185–206. https://doi.org/10.1007/978-3-540-68046-8_6

Fichtner A, Villaseñor A (2015) Crust and upper mantle of the western Mediterranean—constraints from full-waveform inversion. Earth Planet Sci Lett 428:52–62. https://doi.org/10.1016/j.epsl.2015.07.038

Flowers RM, Shuster DL, Wernicke BP, Farley KA (2007) Radiation damage control on apatite (U-Th)/He dates from the Grand Canyon region. Colorado Plateau Geol 35(5):447. https://doi.org/10.1130/G23471A.1

Frenzel G (1975) Die Nephelingesteinsparagenese des Katzenbuckels im Odenwald. Aufschluß Sonderband 27:213–228

Gerdes A, Zeh A (2006) Combined U-Pb and Hf isotope LA-(MC-) ICP-MS analyses of detrital zircons: Comparison with SHRIMP and new constraints for the provenance and age of an Armorican metasediment in Central Germany. Earth Planet Sci Lett 249(1–2):47–61. https://doi.org/10.1016/j.epsl.2006.06.039

Gerdes A, Zeh A (2009) Zircon formation versus zircon alteration—new insights from combined U-Pb and Lu–Hf in-situ LA-ICP-MS analyses, and consequences for the interpretation of Archean zircon from the Central Zone of the Limpopo Belt. Chem Geol 261(3–4):230–243. https://doi.org/10.1016/j.chemgeo.2008.03.005

Ghobadi M, Brey GP, Gerdes A, Höfer HE, Keller J (2021) Accessories in Kaiserstuhl carbonatites and related rocks as accurate and faithful recorders of whole rock age and isotopic composition. Int J Earth Sci (geol Rundsch). https://doi.org/10.1007/s00531-021-02130-9

Goes S, Spakman W, Bijwaard H (1999) A lower mantle source for central european volcanism. Science 286(5446):1928–1931. https://doi.org/10.1126/science.286.5446.1928

Granet M, Wilson M, Achauer U (1995) Imaging a mantle plume beneath the French Massif Central. Earth Planet Sci Lett 136(3–4):281–296. https://doi.org/10.1016/0012-821X(95)00174-B

Gregor H-J (2003) Miocene macroflora of Randecker Maar (Germany). PANGAEA. https://doi.org/10.1594/PANGAEA.104847

Griesshaber E, O'Nions RK, Oxburgh ER, (1992) Helium and carbon isotope systematics in crustal fluids from the Eifel, the Rhine Graben and Black Forest, F.R.G. Chem Geol 99(4):213–235. https://doi.org/10.1016/0009-2541(92)90178-8

Grimm KI (2011) Stratigraphie von Deutschland IX. Tertiär, Teil 1: Oberrheingraben und benachbarte Tertiärgebiete. Schriftenreihe der Deutschen Gesellschaft für Geowissenschaften, vol 75. Schweizerbart, Stuttgart

Grimmer JC, Ritter JRR, Eisbacher GH, Fielitz W (2017) The Late Variscan control on the location and asymmetry of the Upper Rhine Graben. Int J Earth Sci (geol Rundsch) 106(3):827–853. https://doi.org/10.1007/s00531-016-1336-x

Haase KM, Goldschmidt B, Garbe-Schönberg C-D (2004) Petrogenesis of Tertiary continental Intra-plate Lavas from the Westerwald Region. Germany J Petrol 45(5):883–905. https://doi.org/10.1093/petrology/egg115

Harangi S, Molnár M, Vinkler AP, Kiss B, Jull AJT, Leonard AG (2010) Radiocarbon dating of the last volcanic eruptions of Ciomadul Volcano, southeast Carpathians. Eastern-Central Europe Radiocarb 52(3):1498–1507. https://doi.org/10.1017/S0033822200046580

Harangi S, Lukács R, Schmitt AK, Dunkl I, Molnár K, Kiss B, Seghedi I, Novothny Á, Molnár M (2015) Constraints on the timing of Quaternary volcanism and duration of magma residence at Ciomadul volcano, east–central Europe, from combined U-Th/He and U–Th zircon geochronology. J Volcanol Geotherm Res 301:66–80. https://doi.org/10.1016/j.jvolgeores.2015.05.002

Harmon RS, Hoefs J, Wedepohl KH (1987) Stable isotope (O, H, S) relationships in Tertiary basalts and their mantle xenoliths from the Northern Hessian Depression, W. Germany. Contrib Mineral Petrol 95(3):350–369. https://doi.org/10.1007/BF00371849

Heaman L, Parrish RR (1991) U-Pb geochronology on accessory minerals. In: Ludden JN (ed) Heaman L. Applications of radiogenic isotope systems to problems in geology, Toronto, pp 59–102

Hegner E, Vennemann TW (1997) Role of fluids in the origin of Tertiary European intraplate volcanism: Evidence from O, H, and Sr isotopes in melilitites. Geol 25(11):1035. https://doi.org/10.1130/0091-7613(1997)025%3c1035:ROFITO%3e2.3.CO;2

Hegner E, Walter HJ, Satir M (1995) Pb-Sr-Nd isotopic compositions and trace element geochemistry of megacrysts and melilitites from the Tertiary Urach volcanic field: source composition of small volume melts under SW Germany. Contrib Mineral Petrol 122(3):322–335. https://doi.org/10.1007/s004100050131

Heidbach O, Custodio S, Kingdon A, Mariucci MT, Montone P, Müller B, Pierdominici S, Rajabi M, Reinecker J, Reiter K, Tingay M, Williams J, Ziegler M (2016) Stress map of the mediterranean and central Europe 2016. GFZ Data Services. https://doi.org/10.5880/WSM.Europe2016

Hoffmann M (2017) Young tectonic evolution of the Northern Alpine Foreland Basin, southern Germany, based on linking geomorphology and structural geology, Dissertation, Ludwig Maximilian University of Munich. https://edoc.ub.uni-muenchen.de/21123/1/Hoffmann_Markus.pdf

Horn P, Lippolt HJ, Todt W (1972) Kalium-Argon-Altersbestimmungen an tertiären Vulkaniten des Oberrheingrabens. Teil I, Gesamtgesteinsalter. Eclogae Geol Helv 65(1):131–156

Horstwood MSA, Košler J, Gehrels G, Jackson SE, McLean NM, Paton C, Pearson NJ, Sircombe K, Sylvester P, Vermeesch P, Bowring JF, Condon DJ, Schoene B (2016) Community-derived standards for LA-ICP-MS U-(Th-)Pb geochronology—uncertainty propagation, age interpretation and data reporting. Geostand Geoanal Res 40(3):311–332. https://doi.org/10.1111/j.1751-908X.2016.00379.x

Hurai V, Danišík M, Huraiová M, Paquette J-L, Ádám A (2013) Combined U/Pb and (U–Th)/He geochronometry of basalt maars in Western Carpathians: implications for age of intraplate volcanism and origin of zircon metasomatism. Contrib Mineral Petrol 166(4):1235–1251. https://doi.org/10.1007/s00410-013-0922-1

Hurrle H (1976) Ocelli- und Mandelbildung der ultrabasischen Basalte im Kalisalzlager Buggingen und im Kristallin des Schwarzwaldes. Jahresh Geol Landesamt Baden-Wurtt 18:19–37

Jackson SE, Pearson NJ, Griffin WL, Belousova EA (2004) The application of laser ablation-inductively coupled plasma-mass spectrometry to in situ U-Pb zircon geochronology. Chem Geol 211(1–2):47–69. https://doi.org/10.1016/j.chemgeo.2004.06.017

Jung S, Hoernes S (2000) The major- and trace-element and isotope (Sr, Nd, O) geochemistry of Cenozoic alkaline rift-type volcanic rocks from the Rhön area (central Germany): petrology, mantle source characteristics and implications for asthenosphere–lithosphere interactions. J Volcanol Geotherm Res 99(1–4):27–53. https://doi.org/10.1016/S0377-0273(00)00156-6

Jung S, Pfänder JA, Brügmann G, Stracke A (2005) Sources of primitive alkaline volcanic rocks from the Central European Volcanic Province (Rhön, Germany) inferred from Hf, Os and Pb isotopes. Contrib Mineral Petrol 150(5):546–559. https://doi.org/10.1007/s00410-005-0029-4

Jung C, Jung S, Hoffer E, Berndt J (2006) Petrogenesis of Tertiary Mafic Alkaline Magmas in the Hocheifel. Germany J Petrol 47(8):1637–1671. https://doi.org/10.1093/petrology/egl023

Jung S, Pfänder JA, Brauns M, Maas R (2011) Crustal contamination and mantle source characteristics in continental intra-plate volcanic rocks: Pb, Hf and Os isotopes from central European volcanic province basalts. Geochim Cosmochim Acta 75(10):2664–2683. https://doi.org/10.1016/j.gca.2011.02.017

Jung S, Mezger K, Hauff F, Pack A, Hoernes S (2013) Petrogenesis of rift-related tephrites, phonolites and trachytes (Central European Volcanic Province, Rhön, FRG): Constraints from Sr, Nd, Pb and O isotopes. Chem Geol 354:203–215. https://doi.org/10.1016/j.chemgeo.2013.06.026

Keller J, Kraml M, Henjes-Kunst F (2002) $^{40}Ar/^{39}Ar$ single crystal laser dating of early volcanism in the Upper Rhine Graben and tectonic implications. Schweiz Mineral Petrogr Mitt 82:121–130

Keller J, Brey GP, Lorenz V, Sachs P (1990) IAVCEI 1990 pre-conference excursion 2A: volcanism and petrology of the Upper Rhinegraben (Urach-Hegau-Kaiserstuhl), Mainz

Koban CG, Schweigert G (1993) Microbial Origin of Travertine Fabrics - Two Examples from Southern Germany (Pleistocene Stuttgart Travertines and Miocene Riedöschingen Travertine). Facies 29:251–264. https://doi.org/10.1007/BF02536931

Kolb M, Paulick H, Kirchenbaur M, Münker C (2012) Petrogenesis of Mafic to Felsic Lavas from the Oligocene Siebengebirge Volcanic Field (Germany): implications for the origin of intracontinental volcanism in Central Europe. J Petrol 53(11):2349–2379. https://doi.org/10.1093/petrology/egs053

Kraml M, Keller J, Henjes-Kunst F (1999) Time constraints for the carbonatic intrusions of the Kaiserstuhl volcanic complex, Upper Rhine Graben. Germany J Conf Abstr 4:322

Kraml M, Pik R, Rahn M, Selbekk R, Carignan J, Keller J (2006) A New Multi-Mineral Age Reference Material for $^{40}Ar/^{39}Ar$, (U-Th)/He and Fission Track Dating Methods: the Limberg t3 Tuff. Geostand Geoanalyt Res 30(2):73–86. https://doi.org/10.1111/j.1751-908X.2006.tb00914.x

Kraml M, Keller J, Henjes-Kunst F (1995) New K-Ar, ^{40}Ar-39Ar step heating and ^{40}Ar-^{39}Ar Iaser fusion dates for the Kaiserstuhl volcanic complex. Eur. J. Mineral. (Ber. Dtsch. mineral. Ges.) 7(Beih. 1):142

Kramm U, Wedepohl KH (1990) Tertiary basalts and peridotite xenoliths from the Hessian Depression (NW Germany), reflecting mantle compositions low in radiogenic Nd and Sr. Contrib Mineral Petrol 106(1):1–8. https://doi.org/10.1007/BF00306404

Krause O, Weiskirchner W (1981) Die Olivin-Nephelinite des Hegaus. Jahresh Geol Landesamt Baden-Wurtt 23:87–130

Kröchert JS, Theye T, Buchner E (2009) Considerations on the age of the Urach volcanic field (Southwest Germany). Z Dtsch Ges Geowiss 160(4):325–331. https://doi.org/10.1127/1860-1804/2009/0160-0325

Lenz OK, Wilde V, Mertz DF, Riegel W (2015) New palynology-based astronomical and revised $^{40}Ar/^{39}Ar$ ages for the Eocene maar lake of Messel (Germany). Int J Earth Sci (geol Rundsch) 104(3):873–889. https://doi.org/10.1007/s00531-014-1126-2

Lexa J, Seghedi I, Németh K, Szakács A, Konečny V, Pécskay Z, Fülöp A, Kovacs M (2010) Neogene-Quaternary Volcanic forms in the Carpathian-Pannonian Region: a review. Open Geosci. https://doi.org/10.2478/v10085-010-0024-5

Link K (2010) Die thermo-tektonische Entwicklung des Oberrheingraben-Gebietes seit der Kreide. Dissertation, University of Freiburg

Linthout K, Paulick H, Wijbrans JR (2009) Provenance of basalt blocks from Roman sites in Vleuten-De Meern (the Netherlands) traced to the Tertiary Siebengebirge (Germany): a geoarchaeological quest using petrological and geochemical methods. Neth J Geosci 88(1):55–74. https://doi.org/10.1017/S0016774600000998

Lippolt HJ, Gentner W, Wimmenauer W (1963) Altersbestimmungen nach der Kalium-Argon-Methode an tertiären Eruptivgesteinen Südwestdeutschlands. Jahresh Geol Landesamt Baden-Wurtt 6:507–538

Lippolt HJ, Todt W, Baranyi I (1973) K-Ar ages of basaltic rocks from the Urach volcanic district, SW Germany. Fortschr Mineral Beih 50(3):101–102

Lippolt HJ, Baranyi I, Todt W (1975) Die Kalium-Argon-Alter der postpermischen Vulkanite des nord-östlichen Oberrheingrabens. Aufschluß Sonderbd 27:205–212

Lippolt HJ (1983) Distribution of volcanic activity in space and time. In: Fuchs K, Gehlen K von, Mälzer H, Murawski H, Semmel A (eds) Plateau Uplift. The Rhenish Shield—a case history, 1st edn. Springer, Berlin, pp 112–120

Ludwig KR (2009) Isoplot Version 3.71, a Geochronological Toolkit for Microsoft Excel, 4. Berkeley Geochronol Cent Spec Publ 70

Lukács R, Harangi S, Guillong M, Bachmann O, Fodor L, Buret Y, Dunkl I, Sliwinski J, von Quadt A, Peytcheva I, Zimmerer M (2018) Early to Mid-Miocene syn-extensional massive silicic volcanism in the Pannonian Basin (East-Central Europe): eruption chronology, correlation potential and geodynamic implications. Earth-Sci Rev 179:1–19. https://doi.org/10.1016/j.earscirev.2018.02.005

Lustrino M, Carminati E (2007) Phantom plumes in Europe and the circum-Mediterranean region. In: Foulger GR, Jurdy DM (eds) Plates, plumes, and planetary processes: Geological Society of America Special Paper, vol 430, pp 723–745. https://doi.org/10.1130/2007.2430(33)

Lustrino M, Wilson M (2007) The circum-Mediterranean anorogenic Cenozoic igneous province. Earth-Sci Rev 81(1–2):1–65. https://doi.org/10.1016/j.earscirev.2006.09.002

Lutz H, Lorenz V, Engel T, Häfner F, Haneke J (2013) Paleogene phreatomagmatic volcanism on the western main fault of the northern Upper Rhine Graben (Kisselwörth diatreme and Nierstein-Astheim Volcanic System. Bull Volcanol, Germany). https://doi.org/10.1007/s00445-013-0741-2

Mader S, Ritter JRR, Reicherter K, AlpArray Working Group (2021) Seismicity and seismotectonics of the Albstadt Shear Zone in the northern Alpine foreland. Solid Earth 12(6):1389–1409. https://doi.org/10.5194/se-12-1389-2021

Mahfoud RF, Beck JN (1989) Alkaline basalt-phonolite rocks from the Singen area, Hegau, southern F.R.G. Chem Geol 74(3–4):217–227. https://doi.org/10.1016/0009-2541(89)90033-8

Le Maitre RW, Streckeisen A, Zanettin B, Le Bas MJ, Bonin B, Bateman P, Bellieni G, Dudek A, Efremov S, Keller J, Lameyre J, Sabine PA, Schmid R, Sørensen H, Woolley AR (2002) Igneous rocks. A classification and glossary of terms, 2nd edn. Cambridge University Press, Cambridge. https://doi.org/10.1017/CBO9780511535581

Martha SO, Zulauf G, Dörr W, Nesbor H-D, Petschick R, Prinz-Grimm P, Gerdes A (2014) The Saxothuringian–Rhenohercynian boundary underneath the Vogelsberg volcanic field: evidence from basement xenoliths and U-Pb zircon data of trachyte. Z Dtsch Ges Geowiss 165(3):373–394. https://doi.org/10.1127/1860-1804/2014/0079

Mäussnest O (1974) Die Eruptionspunkte des Schwäbischen Vulkans – Teil I. Z Dtsch Ges Geowiss 125:23–54

Mäussnest O (1975) Die Anomalien des erdmagnetischen Feldes im Gebiet des Katzenbuckels. Aufschluß 27:229–234

Mayer B, Jung S, Romer RL, Pfänder JA, Klügel A, Pack A, Gröner E (2014) Amphibole in alkaline basalts from intraplate settings: implications for the petrogenesis of alkaline lavas from the metasomatised lithospheric mantle. Contrib Mineral Petrol. https://doi.org/10.1007/s00410-014-0989-3

McDowell FW, McIntosh WC, Farley KA (2005) A precise ^{40}Ar–^{39}Ar reference age for the Durango apatite (U–Th)/He and fission-track dating standard. Chem Geol 214(3–4):249–263. https://doi.org/10.1016/j.chemgeo.2004.10.002

Meier L, Eisbacher GH (1991) Crustal kinematics and deep structure of the northern Rhine Graben. Germany Tectonics 10(3):621–630. https://doi.org/10.1029/91TC00142

Merle O (2011) A simple continental rift classification. Tectonophysics 513(1–4):88–95. https://doi.org/10.1016/j.tecto.2011.10.004

Mertz DF, Swisher CC, Franzen JL, Neuffer FO, Lutz H (2000) Numerical dating of the Eckfeld maar fossil site, Eifel, Germany: a calibration mark for the Eocene time scale. Sci Nat (die Naturwissenschaft) 87(6):270–274. https://doi.org/10.1007/s001140050719

Mertz DF, Renne PR, Wuttke M, Mödden C (2007) A numerically calibrated reference level (MP28) for the terrestrial mammal-based biozonation of the European Upper Oligocene. Int J Earth Sci (geol Rundsch) 96(2):353–361. https://doi.org/10.1007/s00531-006-0094-6

Mertz DF, Löhnertz W, Nomade S, Pereira A, Prelević D, Renne PR (2015) Temporal–spatial evolution of low-SiO2 volcanism in the Pleistocene West Eifel volcanic field (West Germany) and relationship to upwelling asthenosphere. J Geodyn 88:59–79. https://doi.org/10.1016/j.jog.2015.04.002

Molnár K, Lukács R, Dunkl I, Schmitt AK, Kiss B, Seghedi I, Szepesi J, Harangi S (2019) Episodes of dormancy and eruption of the Late Pleistocene Ciomadul volcanic complex (Eastern Carpathians, Romania) constrained by zircon geochronology. J Volcanol Geotherm Res 373:133–147. https://doi.org/10.1016/j.jvolgeores.2019.01.025

Mrlina J, Kämpf H, Geissler WH, van den Bogaard P (2007) Assumed Quaternary maar structure at the Czech/German boundary between Mýtina and Neualbenreuth (western Eger Rift, Central Europe): geophysical, petrochemical and geochronological indications. Z Geol Wiss 35(4–5):213–230

Neuhaus S (2010) New age for Paleogene/Neogene clastics at the northern termination of the Upper Rhine Graben (Hesse, Germany). Z Dtsch Ges Geowiss 161(3):303–322. https://doi.org/10.1127/1860-1804/2010/0161-0303

Neumann U, Metz P, Westphal F (1992) Vulkanismus der Schwäbischen Alb. Beih Eur J Mineral 4(2):1–37

Nowell DAG, Jones MC, Pyle DM (2006) Episodic Quaternary volcanism in France and Germany. J Quat Sci 21(6):645–675. https://doi.org/10.1002/jqs.1005

Pfänder JA, Jung S, Münker C, Stracke A, Mezger K (2012) A possible high Nb/Ta reservoir in the continental lithospheric mantle and consequences on the global Nb budget—evidence from continental basalts from Central Germany. Geochim Cosmochim Acta 77:232–251. https://doi.org/10.1016/j.gca.2011.11.017

Pfänder JA, Jung S, Klügel A, Münker C, Romer RL, Sperner B, Rohrmüller J (2018) Recurrent local melting of metasomatised lithospheric mantle in response to continental rifting: constraints from Basanites and Nephelinites/Melilitites from SE Germany. J Petrol 59(4):667–694. https://doi.org/10.1093/petrology/egy041

Przybyla T, Pfänder JA, Münker C, Kolb M, Becker M, Hamacher U (2018) High-resolution $^{40}Ar/^{39}Ar$ geochronology of volcanic rocks from the Siebengebirge (Central Germany)—implications for eruption timescales and petrogenetic evolution of intraplate volcanic fields. Int J Earth Sci (geol Rundsch) 107(4):1465–1484. https://doi.org/10.1007/s00531-017-1553-y

Puziewicz J, Matusiak-Małek M, Ntaflos T, Grégoire M, Kaczmarek M-A, Aulbach S, Ziobro M, Kukuła A (2020) Three major types of subcontinental lithospheric mantle beneath the Variscan orogen in Europe. Lithos 362–363:105467. https://doi.org/10.1016/j.lithos.2020.105467

Rasser MW, Bechly G, Böttcher R, Ebner M, Heizmann E, Höltke O, Joachim C, Kern AK, Kovar-Eder J, Nebelsick JH, Roth-Nebelsick A, Schoch RR, Schweigert G, Ziegler R (2013) The Randeck Maar: palaeoenvironment and habitat differentiation of a Miocene lacustrine system. Palaeogeogr Palaeoclimatol Palaeoecol 392:426–453. https://doi.org/10.1016/j.palaeo.2013.09.025

Riisager J, Perrin M, Riisager P, Ruffet G (2000) Paleomagnetism, paleointensity and geochronology of Miocene basalts and baked sediments from Velay Oriental. French Massif Central J Geophys Res 105(B1):883–896. https://doi.org/10.1029/1999JB900337

Ring U, Bolhar R (2020) Tilting, uplift, volcanism and disintegration of the South German block. Tectonophysics 795:228611. https://doi.org/10.1016/j.tecto.2020.228611

Ring U, Gerdes A (2016) Kinematics of the Alpenrhein-Bodensee graben system in the Central Alps: Oligocene/Miocene transtension due to formation of the Western Alps arc. Tectonics 35(6):1367–1391. https://doi.org/10.1002/2015TC004085

Ritter JR, Jordan M, Christensen UR, Achauer U (2001) A mantle plume below the Eifel volcanic fields. Germany Earth Planet Sci Lett 186(1):7–14. https://doi.org/10.1016/S0012-821X(01)00226-6

Rupf I, Nitsch E (2008) Das Geologische Landesmodell von Baden-Württemberg: Datengrundlagen, technische Umsetzung und erste geologische Ergebnisse. LGRB-Inf 21:1–81

Schleicher H, Keller J, Kramm U (1990) Isotope studies on alkaline volcanics and carbonatites from the Kaiserstuhl, Federal Republic of Germany. Lithos 26:21–35. https://doi.org/10.1016/0024-4937(90)90038-3

Schmitt AK (2006a) Hochauflösende U-Pb Datierung von Zirkonen des Sporneiche Trachyts. Geol Jahrb Hess 133:75–81

Schmitt AK (2006b) Laacher See revisited: high-spatial-resolution zircon dating indicates rapid formation of a zoned magma chamber. Geol 34(7):597. https://doi.org/10.1130/G22533.1

Schmitt AK, Marks MA, Nesbor HD, Markl G (2007) The onset and origin of differentiated Rhine Graben volcanism based on U-Pb ages and oxygen isotopic composition of zircon. Eur J Mineral 19(6):849–857. https://doi.org/10.1127/0935-1221/2007/0019-1776

Schmitt AK, Wetzel F, Cooper KM, Zou H, Wörner G (2010) Magmatic longevity of Laacher See Volcano (Eifel, Germany) indicated by U-Th dating of intrusive carbonatites. J Petrol 51(5):1053–1085. https://doi.org/10.1093/petrology/egq011

Schmitt AK, Klitzke M, Gerdes A, Schäfer C (2017) Zircon Hafnium-oxygen isotope and trace element petrochronology of intraplate volcanic rocks from the Eifel (Germany) and implications for Mantle versus crustal origins of zircon megacrysts. J Petrol 58(9):1841–1870. https://doi.org/10.1093/petrology/egx075

Schreiner A (1965) Die Juranagelfluh im Hegau. Jahreshefte Des Geologischen Landesamtes Baden-Württemberg 7:303–354

Schubert S, Jung S, Pfänder JA, Hauff F, Garbe-Schönberg D (2015) Petrogenesis of Tertiary continental intra-plate lavas between Siebengebirge and Westerwald, Germany: constraints from trace element systematics and Nd, Sr and Pb isotopes. J Volcanol Geotherm Res 305:84–99. https://doi.org/10.1016/j.jvolgeores.2015.08.023

Schumacher ME (2002) Upper Rhine Graben: role of preexisting structures during rift evolution. Tectonics 21(1):1006. https://doi.org/10.1029/2001TC900022

Seghedi I, Downes H (2011) Geochemistry and tectonic development of Cenozoic magmatism in the Carpathian–Pannonian region. Gondwana Res 20(4):655–672

Shaw CSJ, Woodland AB, Hopp J, Trenholm ND (2010) Structure and evolution of the Rockeskyllerkopf Volcanic Complex, West Eifel Volcanic Field. Germany Bull Volcanol 72(8):971–990. https://doi.org/10.1007/s00445-010-0380-9

Singer BS, Hoffman KA, Schnepp E, Guillou H (2008) Multiple Brunhes Chron excursions recorded in the West Eifel (Germany) volcanics: support for long-held mantle control over the non-axial dipole field. Phys Earth Planet Inter 169(1–4):28–40. https://doi.org/10.1016/j.pepi.2008.05.001

Sirocko F, Dietrich S, Veres D, Grootes PM, Schaber-Mohr K, Seelos K, Nadeau M-J, Kromer B, Rothacker L, Röhner M, Krbetschek M, Appleby P, Hambach U, Rolf C, Sudo M, Grim S (2013) Multi-proxy dating of Holocene maar lakes and Pleistocene dry maar sediments in the Eifel, Germany. Quat Sci Rev 62:56–76. https://doi.org/10.1016/j.quascirev.2012.09.011

Skála R, Ulrych J, Ackerman L, Krmíček L, Fediuk F, Balogh K, Hegner E (2015) Upper Cretaceous to Pleistocene melilitic volcanic rocks of the Bohemian Massif: petrology and mineral chemistry. Geol Carp 66(3):197–216. https://doi.org/10.1515/geoca-2015-0020

Spear FS, Parrish RR (1996) Petrology and cooling rates of the Valhalla complex, British Columbia. Canada J Petrol 37(4):733–765. https://doi.org/10.1093/petrology/37.4.733

Staesche A (1995) Der genetische Zusammenhang zwischen Melilithiten und Phonolithen des Hegaus, SW-Deutschland. Diploma thesis, University of Tübingen

Stähle V, Koch M (2003) Primary and secondary pseudobrookite minerals in volcanic rocks from the Katzenbuckel Alkaline Complex, southwestern Germany. Swiss Bull Mineral Petrol 83(2):145–158

Stellrecht R, Emmermann R (1970) Das Olivinnephelinit-Vorkommen von Forst/Pfalz. Oberrh Geol Abh 19:29–41

Sundermeyer C, Gätjen J, Weimann L, Wörner G (2020) Timescales from magma mixing to eruption in alkaline volcanism in the Eifel volcanic fields, western Germany. Contrib Mineral Petrol. https://doi.org/10.1007/s00410-020-01715-y

Tappe S, Simonetti A (2012) Combined U-Pb geochronology and Sr–Nd isotope analysis of the Ice River perovskite standard, with implications for kimberlite and alkaline rock petrogenesis. Chem Geol 304–305:10–17. https://doi.org/10.1016/j.chemgeo.2012.01.030

Tera F, Wasserburg GJ (1972) U-Th-Pb systematics in three Apollo 14 basalts and the problem of initial Pb in lunar rocks. Earth Planet Sci Lett 14(3):281–304. https://doi.org/10.1016/0012-821X(72)90128-8

Thomson SN, Zeh A (2000) Fission-track thermochronology of the Ruhla Crystalline Complex: new constraints on the post-Variscan thermal evolution of the NW Saxo-Bohemian Massif. Tectonophysics 324(1–2):17–35. https://doi.org/10.1016/S0040-1951(00)00113-X

Timar-Geng Z, Fügenschuh B, Wetzel A, Dresmann H (2006) Low-temperature thermochronology of the flanks of the southern Upper Rhine Graben. Int J Earth Sci (geol Rundsch) 95(4):685–702. https://doi.org/10.1007/s00531-005-0059-1

Ulrych J, Dostal J, Hegner E, Balogh K, Ackerman L (2008) Late Cretaceous to Paleocene melilitic rocks of the Ohře/Eger Rift in northern Bohemia, Czech Republic: Insights into the initial stages of continental rifting. Lithos 101(1–2):141–161. https://doi.org/10.1016/j.lithos.2007.07.012

Ulrych J, Dostal J, Adamovič J, Jelínek E, Špaček P, Hegner E, Balogh K (2011) Recurrent Cenozoic volcanic activity in the Bohemian Massif (Czech Republic). Lithos 123(1–4):133–144. https://doi.org/10.1016/j.lithos.2010.12.008

Ulrych J, Ackerman L, Balogh K, Hegner E, Jelínek E, Pécskay Z, Přichystal A, Upton BG, Zimák J, Foltýnová R (2013) Plio-Pleistocene basanitic and melilititic series of the Bohemian Massif: K-Ar ages, major/trace element and Sr–Nd isotopic data. Geochemistry 73(4):429–450. https://doi.org/10.1016/j.chemer.2013.02.001

Ulrych J, Krmíček L, Tomek Č, Lloyd FE, Ladenberger A, Ackerman L, Balogh K (2016) Petrogenesis of Miocene alkaline volcanic suites from western Bohemia: whole rock geochemistry and Sr–Nd–Pb isotopic signatures. Geochemistry 76(1):77–93. https://doi.org/10.1016/j.chemer.2015.11.003

van den Bogaard P (1995) $^{40}Ar/^{39}Ar$ ages of sanidine phenocrysts from Laacher See Tephra (12,900 yr BP): chronostratigraphic and petrological significance. Earth Planet Sci Lett 133:163–174. https://doi.org/10.1016/0012-821X(95)00066-L

Voigt T, Kley J, Voigt S (2021) Dawn and dusk of Late Cretaceous basin inversion in central Europe. Solid Earth 12(6):1443–1471. https://doi.org/10.5194/se-12-1443-2021

von Eynatten H, Dunkl I, Brix M, Hoffmann V-E, Raab M, Thomson SN, Kohn B (2019) Late Cretaceous exhumation and uplift of the Harz Mountains, Germany: a multi-method thermochronological approach. Int J Earth Sci (geol Rundsch) 108(6):2097–2111. https://doi.org/10.1007/s00531-019-01751-5

von Eynatten H, Kley J, Dunkl I, Hoffmann V-E, Simon A (2021) Late Cretaceous to Paleogene exhumation in Central Europe—localized inversion vs. large-scale domal uplift. Solid Earth 12:935–958. https://doi.org/10.5194/se-12-935-2021

Wagner GA (1976) Spaltspurendatierungen an Apatit und Titanit aus den Subvulkaniten des Kaiserstuhls. N Jahrb Mineral Monatshefte 9:389–393

Wagner GA, Gögen K, Jonckheere R, Kämpf H, Wagner I, Woda C (1998) The age of Quaternary volcanoes Železná Hůrka and Komurni Hůrka (western Eger Rift), Czech Republic Republic: Alpha-recoil Track, TL, ESR and Fission Track chronometry. In: Cajz V, Adomoviè J (eds) Ulrych J. Magmatism and rift basin evolution, Prague, pp 95–96

Wagner GA, Michalski I, Zaun P (1989) Apatite fission track dating of the Central European basement. Postvariscan Thermo-Tectonic Evolution. In: Emmermann R, Wohlenberg J (eds) The German continental deep drilling program (KTB). Site-selection Studies in the Oberpfalz and Schwarzwald. Springer, Berlin, Heidelberg, pp 481–500

Walter BF, Gerdes A, Kleinhanns IC, Dunkl I, von Eynatten H, Kreissl S, Markl G (2018) The connection between hydrothermal fluids, mineralization, tectonics and magmatism in a continental rift setting: fluorite Sm-Nd and hematite and carbonates U-Pb geochronology from the Rhinegraben in SW Germany. Geochim Cosmochim Acta 240:11–42. https://doi.org/10.1016/j.gca.2018.08.012

Wedepohl KH, Baumann A (1999) Central European Cenozoic plume volcanism with OIB characteristics and indications of a lower mantle source. Contrib Mineral Petrol 136(3):225–239. https://doi.org/10.1007/s004100050534

Wedepohl KH, Gohn E, Hartmann G (1994) Cenozoic alkali basaltic magmas of western Germany and their products of differentiation. Contrib Mineral Petrol 115(3):253–278. https://doi.org/10.1007/BF00310766

Wijbrans J, Németh K, Martin U, Balogh K (2007) $^{40}Ar/^{39}Ar$ geochronology of Neogene phreatomagmatic volcanism in the western Pannonian Basin. Hung J Volcanol Geotherm Res 164(4):193–204. https://doi.org/10.1016/j.jvolgeores.2007.05.009

Wilson M, Downes H (1992) Mafic alkaline magmatism associated with the European Cenozoic rift system. Tectonophysics 208:173–182. https://doi.org/10.1016/B978-0-444-89912-5.50014-4

Witt-Eickschen G, Kramm U (1998) Evidence for the multiple stage evolution of the subcontinental lithospheric mantle beneath the Eifel (Germany) from pyroxenite and composite pyroxenite/peridotite xenoliths. Contrib Mineral Petrol 131(2–3):258–272. https://doi.org/10.1007/s004100050392

Wörner G, Zindler A, Staudigel H, Schmincke H-U (1986) Sr, Nd, and Pb isotope geochemistry of Tertiary and Quaternary alkaline volcanics from West Germany. Earth Planet Sci Lett 79:107–119. https://doi.org/10.1016/0012-821X(86)90044-0

Wu F-Y, Yang Y-H, Mitchell RH, Li Q-L, Yang J-H, Zhang Y-B (2010) In situ U-Pb age determination and Nd isotopic analysis of perovskites from kimberlites in southern Africa and Somerset Island. Canada Lithos 115(1–4):205–222. https://doi.org/10.1016/j.lithos.2009.12.010